

Fetal Physiologically Based Pharmacokinetic Models: Systems Information on the Growth and Composition of Fetal Organs

Khaled Abduljalil¹  · Masoud Jamei¹ · Trevor N. Johnson¹

Published online: 10 July 2018

© Springer International Publishing AG, part of Springer Nature 2018

Abstract

Background The growth of fetal organs is a dynamic process involving considerable changes in the anatomical and physiological parameters that can alter fetal exposure to xenobiotics in utero. Physiologically based pharmacokinetic models can be used to predict the fetal exposure as time-varying parameters can easily be incorporated.

Objective The objective of this study was to collate, analyse and integrate the available time-varying parameters needed for the physiologically based pharmacokinetic modelling of xenobiotic kinetics in a fetal population.

Methods We performed a comprehensive literature search on the physiological development of fetal organs. Data were carefully assessed, integrated and a meta-analysis was performed to establish growth trends with fetal age and weight. Algorithms and models were generated to describe the growth of these parameter values as functions of age and/or weight.

Results Fetal physiologically based pharmacokinetic parameters, including the size of the heart, liver, brain, kidneys, lungs, spleen, muscles, pancreas, skin, bones, adrenal and thyroid glands, thymus, gut and gonads were quantified as a function of fetal age and weight. Variability around the means of these parameters at different fetal ages was also reported. The growth of the investigated

parameters was not consistent (with respect to direction and monotonicity).

Conclusion Despite the limitations identified in the availability of some values, the data presented in this article provide a unique resource for age-dependent organ size and composition parameters needed for fetal physiologically based pharmacokinetic modelling. This will facilitate the application of physiologically based pharmacokinetic models during drug development and in the risk assessment of environmental chemicals and following maternally administered drugs or unintended exposure to environmental toxicants in this population.

Key Points

Data on the growth and composition of human fetal organs are available from different publications.

Collating and mathematically describing these organs during in utero development are important for building fetal physiologically based pharmacokinetic models.

A combined maternal-fetal physiologically based pharmacokinetic model can be used to describe fetal exposure to drugs and possible toxicity in the unborn child after maternal drug intake.

Electronic supplementary material The online version of this article (<https://doi.org/10.1007/s40262-018-0685-y>) contains supplementary material, which is available to authorized users.

✉ Khaled Abduljalil
khaled.abduljalil@certara.com

¹ Certara UK Limited (Simcyp), Level 2-Acero, 1 Concourse Way, Sheffield S1 2BJ, UK

1 Introduction

The use of fetal physiologically based pharmacokinetic (PBPK) models to predict exposure to xenobiotics is an emerging research area [1, 2]. However, such models require comprehensive information on the physiological and biochemical variables describing the growth and composition of fetal organs during development.

In-utero growth of the human foetus body occurs at various rates. The *embryonic period*, which is characterised by extensive cell differentiation through different stages of organ formation (organogenesis), is considered to last up to 8 weeks [3]. The process of organogenesis takes several weeks before individual organs become detectable by ultrasonography or other techniques. There is not a distinct developmental process that marks the end of the embryonic period and the beginning of the fetal period. During the *fetal period*, from week 9 to birth [4], organs become visible and quantifiable. They grow at different rates with each having a varying contribution to the total body weight.

Xenobiotics can perturb normal organ development and function [5–7], while in turn the complex physiological changes alter drug disposition in both the maternal and fetal body. Human foetuses are exposed to prescription and non-prescription drugs antenatally or during labour as well as from unintended exposure to environmental toxicants. Such exposure can harm the foetus when these drugs reach fetal circulation. For example, maternal administration of diethylstilbestrol and other synthetic estrogens disorganises the developing uterine muscle layers and has been linked to the occurrence of genital adenocarcinoma and deformity of the female offspring [8, 9], while nonsteroidal anti-inflammatory drugs can impair both renal structure and function in the foetus [10] causing lifelong consequences such as hypertension [11]. Other drugs such as methotrexate can cause fetal death, teratogenic effects and miscarriage when administered to a pregnant woman during organogenesis [12, 13].

Therefore, evaluation of drug and metabolite exposure in the fetal body during the early gestation time when organogenesis takes place can improve our understanding on fetal toxicity. In some medical settings, it is the foetus who is the target of the treatment and adequate fetal drug exposure can contribute to the efficacy of the treatment, as in the case of maternal administration of antiretroviral agents to prevent mother-to-child viral transmission [6], digoxin to treat life-threatening fetal tachyarrhythmias [14] and glucocorticoids to promote fetal lung maturation in cases of threatening premature birth [15]. In some cases, the drug is installed in the amniotic fluid as in the case of

thyroxine supplementation to treat fetal goitrous hypothyroidism [16].

The amount and duration of fetal drug exposure after maternal administration depend on the maternal dosing regimen and is greatly modified by the maternal physiological system, including the placental metabolism and transfer. Because the foeto-maternal physiological changes are not uniform, their effects on each xenobiotic or drug may differ depending on the absorption, distribution, metabolism and excretion characteristics. Fetal PBPK models allow the integration of available anatomical and physiological ‘system’ parameters describing the fetal growth and development, together with ‘drug’ parameters (e.g. physicochemical properties of the drug) to enable the prediction of tissue and plasma exposure. When the fetal PBPK model is combined with the maternal PBPK model, different pharmacological and toxicological scenarios can be predicated.

Anatomical growth for limited fetal organs has been reviewed previously in different publications based on a limited number of autopsy studies and some of these focussed on a limited period of fetal development [17–22]. Since then, many studies with larger sample sizes covering a wider period of fetal age (FA) and using better methodology have been reported. In previous publications, we have reported changes occurring to the maternal body during gestation [23] and have introduced the requirements for the quantification of biometric parameters, mainly, the fetal weight, height and body surface area for both male and female individuals as well as the gross body composition for the development of a fetal PBPK model [24]. Here, we extend this research to include fetal organ size and composition.

The aim of the current article was to review, collate and integrate the available studies on the growth and composition of fetal organs during development to extend the database needed for building a fetal PBPK model. This study describes the changes in fetal organs and provides algorithms to be used within fetal PBPK models.

2 Methods

2.1 Data Sources

We conducted a structured comprehensive literature search of MEDLINE for embryo/fetal tissue growth and composition parameters during development. The search strategy was aimed to identify observational cohort studies in which the required parameters were longitudinally examined during fetal development. For each parameter, a separate search was conducted, using the keyword ‘fetal or fetal’ plus the parameter of interest, for example ‘liver weight’,

‘liver volume’, ‘liver mass’, ‘liver water’, ‘liver composition’, ‘development’ and ‘growth’. No language or date restriction was applied. Article titles and abstracts were screened to maintain the focus of the search upon human pregnancies and the development of fetal organs. A manual search of reference lists from selected articles and contact with experts in the field complemented the data collection process.

2.2 Inclusion Criteria

Data inclusion criteria were (1) singleton, and where possible, low-risk uncomplicated pregnancy with no underlying maternal/fetal conditions that are known to affect the parameters, (2) where possible, foetuses with no major congenital abnormalities for organ weights, (3) in the case of mixed-population studies, low-risk foetuses comprised at least 80% of the overall sample size under study for organ sizes, (4) when fetal and preterm data were available, only fetal data were included, (5) tissue composition values from dead foetuses were used if samples were fresh (see the text), (6) data were collected from the Caucasian population (in the case of mixed-population studies, the Caucasian population comprised at least 80% of the overall population) and (7) where Caucasian data for a specific parameter were not available, data from non-Caucasian populations were considered and mentioned within the relevant section.

2.3 Combining Data from Different Studies

Mean parameter values (and variability) stratified for FA groups were available. The overall mean parameter value, \bar{X} , at a particular gestational age (GA), from different studies was combined using Eq. 1:

$$\bar{X} = \frac{\sum_{j=1}^J n_j x_j}{\sum_{j=1}^J n_j}, \quad (1)$$

where n_j is the number of subjects in the j th study and x_j is the mean value from that study. The overall sum of squares was calculated according to Eq. 2:

$$\text{Overall sum of squares} = \sum_{j=1}^J \left[\left[(sd_j)^2 + (x_j)^2 \right] \cdot n_j \right] - N \cdot \bar{X}^2, \quad (2)$$

where sd_j is the standard deviation from the j th study and N is the number of subjects in all studies ($N = \sum_{j=1}^J n_j$). The overall standard deviation (SD) was calculated according to Eq. 3:

$$\text{Overall SD} = \sqrt{\frac{\text{Overall Sum of Squares}}{N}}. \quad (3)$$

The coefficient of variation (CV) for the weighted mean was then calculated as follows (Eq. 4):

$$\text{CV} = \frac{\text{Overall SD}}{\bar{X}}. \quad (4)$$

In the absence of usable data from the literature, the CV values were assumed to be the same as those for a full-term newborn population.

If the j th study reported mean and standard error, se , at gestational week i th (se_{ji}), the following equation was used to calculate sd_{ji} :

$$sd_{ji} = se_{ji} \cdot \sqrt{n_{ji}}, \quad (5)$$

where n_{ji} is the sample size in the j th study at the i th weeks of age. When data are given as mean and 95% or 90% percentiles, the SD was derived using the following equations using Z scores [25]:

$$\text{SD} = (95\text{th percentile} - \text{mean})/1.645, \quad (6)$$

$$\text{SD} = (90\text{th percentile} - \text{mean})/1.28. \quad (7)$$

2.4 Data Analysis

Before data analysis, when a parameter was reported in different units, these units were converted to a standard unit of measurement. When the age was reported as a range, the midpoint of the interval in weeks was used. When measurements were reported per month for organs only if limited data are available on this organ or if the study included large sample size and provided more information of the studied population and methodology. In these cases, the average month is converted to weeks. If a study report age range only, the median is taken (if no or limited data available for this organ). The details of the data analysis, including methods used to select between rival models, have been described previously [24]. Briefly, common types of growth models were investigated to describe the organ growth data, including linear, polynomial, power, sigmoidal and Weibull functions. Before model testing, data were plotted and visualised for their profiles vs. age and weight. Depending on a visual check of the plotted data only potential models were tested in each case, e.g. for linear data the sigmoidal or power model was dropped. The best fit model was selected by use of the Akaike information criterion (AIC) value. The model with the lowest AIC was selected and if two models had similar AICs, then the simpler model was selected. Data for gut, bone and muscle were limited and hence a simple model was used without challenging the data to different types of

models. Where enough data were available, two sets of equations are provided for each tissue; one a function of age and the second equation a function of body weight. The predicted fetal body weight variability established earlier [24] was used here for each organ to assess if the reported organ variability can be recovered using the body weight variability.

Throughout this article, we use the term ‘fetal age’ to indicate the biological age of the foetus (i.e. post-conceptual age in weeks). The term ‘gestational age’ is used to refer to the post-menstrual age in weeks. Fetal age is calculated by subtracting 2 weeks from the GA reported in original references.

3 Results

The amount of information available on different fetal organ parameters varies considerably depending on the organ. While an abundance of information was available for some organs, e.g. the brain, kidneys and lungs, it was limited for others, e.g. the skin and gut, as seen in the tables of the Electronic Supplementary Material (ESM).

Generally, the data show no marked differences in the size of internal organs between male and female foetuses, supporting previous conclusions [26, 27], and thus the data of both sexes were combined. Where the original studies identified other covariates, we also refer to these findings. Few studies [18, 26, 28, 29] reported their results for organ size in relation to the fetal body weight, these data are mentioned under the relevant organ. Relevant fetal tissue composition data were collated from 16 publications [30–45].

Table 1 and Fig. 1a, b summarise the results of the meta-analysis of available data on age-dependent organ size in terms of means and SDs, along with population age or sizes and suggested regression equations.

3.1 Heart

The heart is one of the earliest differentiating and functioning organs. It begins to beat between 3 and 4 gestational weeks (GW), with blood flow beginning in the fourth week [4, 46]. Many studies report the size of the heart at different FAs using different measurement techniques. Autopsy and ultrasound studies quantified heart growth at certain ages (Table 1 of the ESM). Results from the meta-analysis of the collected heart growth data at different FAs and body weights are given in Table 1. These data can be described using the following equations:

$$\text{Heart mass(g)} = (0.0889 \cdot \text{FA})^{2.546}, \quad (7)$$

$$\text{Heart mass(g)} = 0.0081 \cdot \text{BW} + 0.0000004 \cdot \text{BW}^2. \quad (8)$$

where FA is the fetal age in weeks and BW is the fetal body weight in grams. The selected power-type age-based equation above was superior to polynomial equation, which predicted negative mass at age less than 10 weeks. It was also superior to the Weibull function (AIC: 83.5 vs. 87.8). Among weight-based equations, the polynomial was slightly superior to other equations (AIC were 31, 43 and 34 for polynomial, linear and power, respectively). Plots of the meta-analysis data are given in Fig. 1 of the ESM. Density of the fetal heart aged 14–42 GA was reported to be about 0.98 g/mL [47]. A value of 1.05 g/mL was reported for adult heart tissue [22].

Available data from wet tissue suggested a slight reduction in water with age from about 86% at the beginning of the second trimester reaching about 84% at term. Lipids and proteins increase from 1.8 and 7.8% at 20 GW up to 2.1 and 11.2% at term, respectively [40, 42–44] (Table 20 of the ESM).

3.2 Brain

Development of the nervous system begins at approximately 2.5 weeks of FA [48, 49]. By the end of week 4, three primary brain vesicles are formed: the forebrain, the midbrain and the hindbrain. Maturation of the human brain in the second half of gestation involves substantial increases in volume, increasing the complexity of the cortical plate, and changes in the molecular and cellular composition of the cerebral mantle tissue zones.

A stereological analysis of 22 normal human fetal brains showed that the total number of cells (including both neurons and glial cells) in the forebrain increases exponentially from 0.3 to 1.3 billion between 13 and 20 GW, reaching about 3.8 billion cells in the newborn infant [50]. Similar trends have been also reported by using a chemical analysis of the DNA contents of 139 brains ranging in age from 10 GW to 7 years [34].

Routinely, fetal head circumference measurement is considered as a surrogate for brain growth [24]. Dobbing and Sands measured the growth and development of the human brain and its parts (forebrain, cerebellum and stem) using fresh samples of whole brain from 139 normal human brains, ranging in age from 10 GW to 7 postnatal years, together with nine adult brains. They concluded that the growth of the brain and its parts shows a sigmoidal relationship with age, with half of the weight achieved during the first year of postnatal age [34].

Studies reporting the size of the brain at different FAs using autopsy and magnetic resonance imaging (MRI) are shown in Table 2 of the ESM. Results from the meta-analysis of the collected brain growth data at different FAs and body weights are given in Table 1. These summary

Table 1 Anatomical parameter values and regression equations needed for fetal organ growth, based on a meta-analysis of the published data

Parameter (unit)	Organ size values from a meta-analysis ^a	Equations for human fetal organs ^c	References
Heart weight (g)	10 weeks: 0.34 ± 0.28 (84%), $n = 45$	$\text{Heart(g)} = (0.0889 \cdot \text{FA})^{2.546}$ $\text{Heart(g)} = 0.0081 \cdot \text{BW} + 0.0000004 \cdot \text{BW}^2$ Density of fetal heart = 0.98 g/mL	[28, 118, 175–187]
	15 weeks: 1.13 ± 0.60 (53%), $n = 131$		
	20 weeks: 3.59 ± 1.47 (41%), $n = 272$		
	25 weeks: 8.27 ± 3.98 (48%), $n = 371$		
	30 weeks: 13.19 ± 4.90 (37%), $n = 703$		
	35 weeks: 17.57 ± 7.89 (45%), $n = 255$		
	38 weeks: 21.56 ± 5.68 (26%), $n = 694$		
	27 g BW: 0.16 ± 0.14 (88%), $n = 30$		
	350 g BW: 2.68 ± 1.03 (37%), $n = 336$		
	1400 g BW: 10.47 ± 3.6 (34%), $n = 728$		
2300 g BW: 17.68 ± 5.73 (32%), $n = 442$			
3500 g BW: 23.13 ± 7.77 (33%), $n = 141$			
Brain weight (g)	10 weeks: 3.81 ± 2.11 (56%), $n = 24$	$\text{Brain(g)} = (0.225 \cdot \text{FA})^{2.793}$ $\text{Brain(g)} = (0.255 \cdot \text{BW})^{0.896}$ Density of the fetal brain = 1.08 g/mL	[118, 177–182, 184, 185, 188, 189]
	15 weeks: 23.13 ± 7.65 (33%), $n = 104$		
	20 weeks: 68.12 ± 15.46 (23%), $n = 227$		
	25 weeks: 119.06 ± 37.71 (32%), $n = 215$		
	30 weeks: 212.31 ± 53.27 (25%), $n = 662$		
	35 weeks: 321.07 ± 86.41 (27%), $n = 170$		
	38 weeks: 383.50 ± 78.13 (20%), $n = 871$		
	16 g BW: 2.51 ± 1.1 (44%), $n = 7$		
	100 g BW: 18.86 ± 4.44 (23%), $n = 68$		
	400 g BW: 63.51 ± 18.46 (29%), $n = 297$		
1000 g BW: 140.3 ± 38.5 (27%), $n = 814$			
2000 g BW: 276.3 ± 74.2 (27%), $n = 207$			
3300 g BW: 402.8 ± 69.6 (17%), $n = 542$			
3600 g BW: 447.1 ± 72.3 (14%), $n = 45$			

Table 1 continued

Parameter (unit)	Organ size values from a meta-analysis ^a	Equations for human fetal organs ^c	References
Liver weight (g)	10 weeks: 1.10 ± 1.20 (114%), n = 21 15 weeks: 7.50 ± 3.20 (43%), n = 92 20 weeks: 22.8 ± 7.30 (32%), n = 195 25 weeks: 43.2 ± 11.3 (26%), n = 233 30 weeks: 70.7 ± 24.4 (35%), n = 665 35 weeks: 107.8 ± 32.9 (31%), n = 226 38 weeks: 135.2 ± 45.1 (33%), n = 613 40 g BW: 1.96 ± 1.12 (57%), n = 69 400 g BW: 21.17 ± 6.44(30%), n = 237 1000 g BW: 47.95 ± 14.66(31%), n = 1155 1900 g BW: 80.48 ± 29.63(37%), n = 470 2700 g BW: 118 ± 35.8(30%), n = 418 3550 g BW: 155 ± 56 (36%), n = 209	Liver (g) = (0.152 · FA) ^{2.8} Liver (g) = (0.063 · BW) ^{0.925} Density of fetal liver = 1.01 g/mL	[107, 118, 177–182, 184, 185, 190]
Kidneys weight (g)	10 weeks: 0.22 ± 0.13 (58%), n = 37 15 weeks: 1.32 ± 0.73 (55%), n = 116 20 weeks: 4.09 ± 1.53 (37%), n = 271 25 weeks: 9.31 ± 4.98 (53%), n = 277 30 weeks: 15.93 ± 5.66 (36%), n = 730 35 weeks: 24.38 ± 9.46 (39%), n = 225 38 weeks: 27.28 ± 8.48 (31%), n = 711 90 g BW: 0.68 ± 0.41 (59%), n = 177 510 g BW: 5.08 ± 1.60 (31%), n = 120 1070 g BW: 10.8 ± 4.4 (41%), n = 711 1690 g BW: 16.9 ± 7.7 (45%), n = 909 2530 g BW: 23.8 ± 8.3 (35%), n = 313 3400 g BW: 29.4 ± 8.4 (28%), n = 489	Kidneys(g) = 0.1246 · FA – 0.0333 · FA ² + 0.0026 · FA ³ – 0.00003 · FA ⁴ [28, 60, 118, 175–185, 191–195] Kidneys(g) = 0.011 · BW – 0.0000007 · BW ² The kidney density is approximately 1.05 g/mL	

Table 1 continued

Parameter (unit)	Organ size values from a meta-analysis ^a	Equations for human fetal organs ^c	References
Pancreas weight (g)	10 weeks: 0.02, n = 6 12 weeks: 0.07 ± 0.02 (31%), n = 28 16 weeks: 0.33 ± 0.60 (180%), n = 123 20 weeks: 0.60 ± 0.92 (152%), n = 197 24 weeks: 1.35 ± 0.76 (57%), n = 69 30 weeks: 2.95 ± 2.15 (73%), n = 160 34 weeks: 3.39 ± 2.3 (68%), n = 184 38 weeks: 5.08 ± 2.58 (51%), n = 344 55 g BW: 0.07 ± 0.02(31%), n = 28 105 g BW: 0.22 ± 0.11 (50%), n = 82 600 g BW: 1.18 ± 0.63 (53%), n = 167 1411 g BW: 2.24 ± 0.81 (36%), n = 137 2440 g BW: 3.44 ± 0.92 (27%), n = 139 3185 g BW: 5.07 ± 1.14 (23%), n = 367	Pancreas (g) = (0.048 · FA) ^{2.73} Pancreas (g) = (0.0018 · BW) ^{0.91} Density for fetal pancreas = 1.04 g/mL (proposed)	[118, 184, 185, 187]
Lungs weight (g)	10 weeks: 1.01 ± 0.60 (60%), n = 46 15 weeks: 4.66 ± 2.04 (44%), n = 131 20 weeks: 12.63 ± 3.73 (30%), n = 503 25 weeks: 25.61 ± 9.94 (39%), n = 310 30 weeks: 40.06 ± 13.30 (33%), n = 819 35 weeks: 49.07 ± 19.94 (41%), n = 213 38 weeks: 59.32 ± 19.74 (33%), n = 707 39 g BW: 1.16 ± 0.94(81%), n = 68 95 g BW: 2.98 ± 1.56(52%), n = 174 510 g BW: 13.7 ± 5.6(41%), n = 337 1030 g BW: 26.0 ± 9.9(38%), n = 910 1500 g BW: 37.6 ± 13.5(36%), n = 836 2500 g BW: 47.9 ± 17.3(36%), n = 432 3040 g BW: 56.1 ± 17.2(31%), n = 565 3550 g BW: 62.0 ± 18.1 (29%), n = 198	Lungs(g) = $\frac{90.042 \cdot \text{FA}^{3.795}}{32.02^{3.795} + \text{FA}^{3.795}}$ Lungs(g) = 0.027 · BW – 0.00000275 · BW ² Density of fetal lung = 1.05 g/mL	[118, 177–185, 196–200]

Table 1 continued

Parameter (unit)	Organ size values from a meta-analysis ^a	Equations for human fetal organs ^c	References
Muscles weight (g) ^b	5 weeks: 0.006 ± 0.005 (80%) 10 weeks: 0.32 ± 0.21 (66%) 15 weeks: 5.47 ± 3.90 (71%) 20 weeks: 38.9 ± 9.1 (23%) 25 weeks: 147.1 ± 41.6 (28%) 30 weeks: 362.4 ± 97.6 (27%) 35 weeks: 672.7 ± 148.8 (22%) 38 weeks: 887.9 ± 160.1 (18%) 1.05 g BW: 0.006 ± 0.005 (80%) 110 g BW: 5.47 ± 3.90 (71%) 1053 g BW: 38.9 ± 9.1 (23%) 2982 g BW: 147.1 ± 41.6 (28%) 3606 g BW: 362.4 ± 97.6 (27%)	$\text{Muscle (g)} = (0.194 \cdot \text{FA})^{3.19}$ $\text{Muscle (g)} = (0.029 \cdot \text{BW})^{1.46}$ Density of fetal muscle = 1.04 g/mL (adult value)	[84, 85] Total n = 41
Spleen weight (g)	10 weeks: 0.02 ± 0.01 (79%), n = 14 15 weeks: 0.14 ± 0.09 (67%), n = 116 20 weeks: 0.62 ± 0.28 (45%), n = 238 25 weeks: 2.29 ± 0.85 (37%), n = 231 30 weeks: 4.86 ± 2.00 (41%), n = 664 35 weeks: 9.28 ± 4.14 (45%), n = 239 38 weeks: 10.5 ± 3.82 (36%), n = 694 40 g BW: 0.03 ± 0.04 (118%), n = 50 160 g BW: 0.18 ± 0.11 (62%), n = 152 470 g BW: 0.70 ± 0.30 (50%), n = 237 1000 g BW: 2.72 ± 1.54 (57%), n = 1126 1710 g BW: 5.25 ± 3.70 (71%), n = 1236 2400 g BW: 8.80 ± 3.43 (39%), n = 785 3450 g BW: 11.37 ± 4.82 (42%), n = 336	$\text{Spleen (g)} = (0.05 \cdot \text{FA})^{3.7}$ $\text{Spleen (g)} = \frac{20.73 \cdot \text{BW}^{1.733}}{30541.733 + \text{BW}^{17.35}}$ Density of fetal spleen = 1.03 g/mL	[28, 107, 118, 177–182, 184, 185, 201]

Table 1 continued

Parameter (unit)	Organ size values from a meta-analysis ^a	Equations for human fetal organs ^c	References
Skin weight (g) ^b	5 weeks: 0.06 ± 0.03 (50%) 10 weeks: 0.97 ± 0.40 (42%) 15 weeks: 6.7 ± 3.0 (45%) 20 weeks: 25.8 ± 4.0 (16%) 25 weeks: 64 ± 12 (19%) 30 weeks: 119 ± 21 (18%) 35 weeks: 182 ± 27 (15%) 38 weeks: 220 ± 26 (12%) 1.05 g BW: 0.06 ± 0.03 (50%) 16.0 g BW: 0.97 ± 0.40 (42%) 110 g BW: 6.7 ± 3.0 (45%) 423 g BW: 25.8 ± 4.0 (16%) 1053 g BW: 64 ± 12 (19%) 1952 g BW: 119 ± 21 (18%) 2982 g BW: 182 ± 27 (15%) 3606 g BW: 220 ± 26 (12%)	$\text{Skin(g)} = (0.1119 \cdot \text{FA})^{3.45}$ $\text{Skin(g)} = 0.061 \cdot \text{BW}$ Density of fetal skin = 1.1 g/mL (proposed)	[19, 90, 123, 202] Total n = 31
Bone weight (g) ^b	5 weeks: 0.11 ± 0.05 (50%) 10 weeks: 1.65 ± 0.68 (52%) 15 weeks: 11.4 ± 5.1 (45%) 20 weeks: 43.8 ± 6.8 (16%) 25 weeks: 109.0 ± 20.3 (19%) 30 weeks: 202.0 ± 35.8 (18%) 35 weeks: 308.6 ± 45.3 (15%) 38 weeks: 373.2 ± 44.9 (12%) 1.05 g BW: 0.11 ± 0.05 (50%) 16.0 g BW: 1.65 ± 0.68 (52%) 110 g BW: 11.4 ± 5.1 (45%) 423 g BW: 43.8 ± 6.8 (16%) 1053 g BW: 109.0 ± 20.3 (19%) 1952 g BW: 202.0 ± 35.8 (18%) 2982 g BW: 308.6 ± 45.3 (15%) 3606 g BW: 373.2 ± 44.9 (12%)	$\text{Bone (g)} = 0.0106 \cdot \text{FA}^3 - 0.2366 \cdot \text{FA}^2 + 3.2253 \cdot \text{FA}$ $\text{Bone (g)} = 0.1035 \cdot \text{BW}$ Density of fetal bone (g/mL) = 1.0 - 0.0028 · FA + 0.0004 · FA ² (proposed)	[37, 103–105, 203]

Table 1 continued

Parameter (unit)	Organ size values from a meta-analysis ^a	Equations for human fetal organs ^c	References
Adrenal glands weight (g)	10 weeks: 0.20 ± 0.24 (118%), n = 30 15 weeks: 0.71 ± 0.43 (61%), n = 115 20 weeks: 1.95 ± 1.13 (58%), n = 387 25 weeks: 2.84 ± 1.17 (41%), n = 284 30 weeks: 4.66 ± 1.99 (43%), n = 705 35 weeks: 6.33 ± 2.67 (42%), n = 226 38 weeks: 8.08 ± 2.85 (35%), n = 916 18 g BW: 0.30 ± 0.24 (83%), n = 12 100 g BW: 0.52 ± 0.30 (57%), n = 57 550 g BW: 2.19 ± 0.87 (40%), n = 361 1030 g BW: 3.69 ± 1.60 (43%), n = 912 1550 g BW: 4.71 ± 1.90 (40%), n = 550 1950 g BW: 5.11 ± 2.11 (41%), n = 415 2890 g BW: 7.64 ± 3.10 (41%), n = 479 3560 g BW: 9.47 ± 3.60 (38%), n = 211	$\text{Adrenal(g)} = (0.063 \cdot \text{FA})^{2.38}$ $\text{Adrenal(g)} = (0.0043 \cdot \text{BW})^{0.81}$ Density of fetal adrenal glands = 0.87 g/mL	[28, 118, 177–182, 184–187]
Thymus weight (g)	10 weeks: 0.04 ± 0.04 (100%), n = 14 15 weeks: 0.18 ± 0.05 (30%), n = 103 20 weeks: 0.88 ± 0.42 (47%), n = 235 25 weeks: 2.49 ± 1.18 (48%), n = 264 30 weeks: 5.54 ± 2.41 (44%), n = 662 35 weeks: 8.84 ± 2.86 (32%), n = 229 38 weeks: 9.59 ± 3.4 (35%), n = 695 33 g BW: 0.04 ± 0.02 (50%), n = 34 125 g BW: 0.16 ± 0.07 (40%), n = 151 400 g BW: 0.81 ± 0.40 (50%), n = 263 700 g BW: 1.82 ± 1.03 (57%), n = 345 1250 g BW: 4.73 ± 2.17 (46%), n = 385 1810 g BW: 6.42 ± 2.67 (42%), n = 696 2400 g BW: 8.08 ± 2.60 (32%), n = 538 3050 g BW: 10.23 ± 3.95 (39%), n = 575 3400 g BW: 11.02 ± 3.81 (35%), n = 273	$\text{Thymus(g)} = \frac{17.89 \cdot \text{FA}^{4.752}}{35.93^{4.752} + \text{FA}^{4.752}}$ $\text{Thymus(g)} = \frac{17.89 \cdot \text{BW}^{1.587}}{2564^{1.587} + \text{BW}^{1.587}}$ Density of fetal thymus = 1.1 g/mL	[28, 118, 177–182, 184, 185, 187]

Table 1 continued

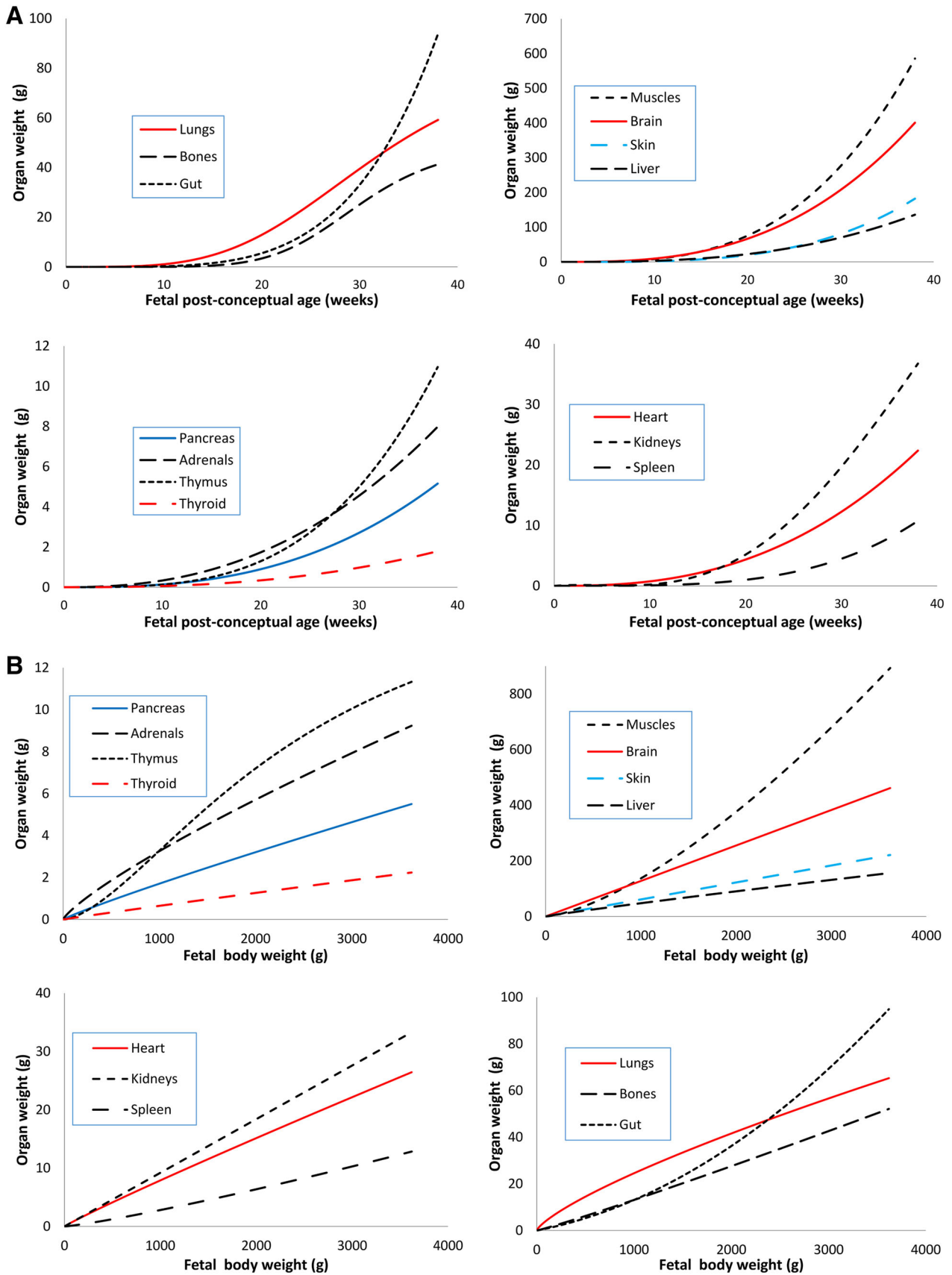
Parameter (unit)	Organ size values from a meta-analysis ^a	Equations for human fetal organs ^c	References
Thyroid weight (g)	13.5 weeks: 0.13 ± 0.08 (62%), n = 19 15.5 weeks: 0.19 ± 0.10 (53%), n = 46 19.5 weeks: 0.33 ± 0.16 (48%), n = 80 25.5 weeks: 0.66 ± 0.25 (38%), n = 21 29.5 weeks: 0.95 ± 0.33 (35%), n = 6 35.5 weeks: 1.54 ± 0.46 (30%), n = 12 37.5 weeks: 1.78 ± 0.51 (29%), n = 26 12 g BW: 0.004 ± 0.002 (50%), n = 10 50 g BW: 0.023 ± 0.010 (43%), n = 8 110 g BW: 0.13 ± 0.08 (62%), n = 19 400 g BW: 0.30 ± 0.16 (54%), n = 97 770 g BW: 0.51 ± 0.22 (42%), n = 58 1300 g BW: 0.80 ± 0.21 (26%), n = 13 2270 g BW: 1.24 ± 0.40 (33%), n = 15 3100 g BW: 1.78 ± 0.51 (29%), n = 26	Thyroid(g) = (0.033 · FA) ^{2.585} Thyroid(g) = (0.00064 · BW) ^{0.96} Density of fetal thyroid gland = 1.05 g/mL (adult value)	[26, 118, 204]
Total gut weight (g) ^b	5 weeks: 0.038 ± 0.006 (16%) 10 weeks: 0.40 ± 0.13 (32%) 15 weeks: 1.83 ± 0.54 (29%) 20 weeks: 5.83 ± 0.79 (14%) 25 weeks: 14.9 ± 2.5 (17%) 30 weeks: 32.81 ± 5.96 (18%) 35 weeks: 65.0 ± 10.2 (16%) 38 weeks: 94.0 ± 11.7 (12%) 1.05 g BW: 0.038 ± 0.006 (16%) 16.0 g BW: 0.40 ± 0.13 (32%) 110 g BW: 1.83 ± 0.54 (29%) 423 g BW: 5.83 ± 0.79 (14%) 1053 g BW: 14.9 ± 2.5 (17%) 1952 g BW: 32.81 ± 5.96 (18%) 2982 g BW: 65.0 ± 10.2 (16%) 3606 g BW: 94.0 ± 11.7 (12%)	GIntact(g) = (0.0737 · FA) ^{4.41} Gut(g) = 0.0081 · BW ² + 0.000005 · BW See the text for the growth of different segment of the gut Density of fetal gut = 1.04 g/mL (adult value)	[134, 149]

BW fetal body weight in grams, FA fetal age in weeks, n number of foetuses

^aValues are expressed as mean ± standard deviation (coefficient of variation)

^bVariability of the organ was propagated from body weight variability

^cDensities in this table can be used to calculate organ volumes. For some organs, no data are available and the proposed ones can be used until clinical data become available



◀ **Fig. 1** Summary plots of the growth of fetal organs needed for a fetal physiologically based pharmacokinetic model as functions of post-conceptual age (a) and body weight (b)

measurements can be described using the following equations:

$$\text{Brain mass(g)} = (0.225 \cdot \text{FA})^{2.793}, \quad (9)$$

$$\text{Brain mass(g)} = (0.255 \cdot \text{BW})^{0.896}. \quad (10)$$

where FA is the post-conception fetal age in weeks and BW is the fetal body weight in grams. The provided age-based function was almost similar to the Weibull function (AIC: 220.7 vs. 221.0), while the weight-based function was superior to the linear model (AIC: 148 vs. 176). Plots of the meta-analysis data against FA and weight are given in Fig. 2 of the ESM.

Mean fetal brain volumes prior to autopsy were compared to their weight at autopsy in 25 foetuses between 16 and 40 GW, and found to be constant during growth with no significant deviation from linearity ($p > 0.10$) [51]. The calculated density of the fetal brain was 1.08 g/mL between 16 and 40 GW ($n = 25$ foetuses) [51]. A value of about 1.03 g/mL was reported for a 1-year old child [52] and 1.04 g/mL for adult brain density [22].

Collected data on fetal brain tissue composition are available from six studies [34, 35, 37, 42, 44, 45] and given in Table 20 of the ESM. Brain water, percentage of wet tissue mass, decreases linearly with FA from the end of the first trimester till birth with an intercept of 93.64% and a negative FA coefficient of 0.1104. Both lipids and protein contents increase about 1.7-fold during this period from 1.5 and 3.8% of the tissue weight.

3.3 Liver

Human liver is the largest internal organ providing essential metabolic, exocrine and endocrine functions. It is quantitatively by far the most important organ for drug metabolism. Most metabolic functions of the fetal liver are handled by the maternal liver, as the fetal liver is primarily a haematopoietic organ until near term [48]. Many liver enzyme systems are still immature at birth and many are not developed by term. A number of metabolising enzymes have been detected in the fetal liver such as cytochrome P450 (CYP)3A7, CYP2C9 and CYP2C8 [53–56], while the other CYPs are present at extremely low levels or totally absent and are thought to develop during the first weeks following birth [56, 57]. Details of enzyme ontogeny and quantifications are beyond the scope of this study.

Studies reporting measurements of the mass of the liver are given in Table 3 of the ESM. A meta-analysis summary of these data at different FAs and body weights is given in Table 1. These summary measurements can be described using the following equations:

$$\text{Liver mass(g)} = (0.152 \cdot \text{FA})^{2.8}, \quad (11)$$

$$\text{Liver mass(g)} = (0.063 \cdot \text{BW})^{0.925}. \quad (12)$$

where FA is the fetal age in weeks and BW is the fetal body weight in grams. The provided age-based function was slightly superior to the Weibull function (AIC: 149 vs. 152), while the weight-based function was clearly superior to the linear model (AIC: 113 vs. 121). Plots of meta-analysis data against FA and weight are given in Fig. 3 of the ESM. A comparison of mean liver volumes before autopsy to their weights at autopsy found a constant linear relationship in 25 foetuses aged 16–40 GW [51].

The calculated density of the fetal liver from 25 foetuses aged 16–40 GW was 1.15 g/mL [51] and 1.01 in foetuses aged 14–42 GW. A value of 1.05 g/mL was reported for an adult [37].

Collected data on fetal liver tissue composition are limited to few samples (Table 20 of the ESM) from five reports [37, 39, 40, 42, 44]. The liver water, as a percentage of wet tissue mass, decreases linearly with FA from the end of the first trimester till birth with an intercept of 85.39% and a negative FA coefficient of 0.1404. Liver protein (13%), lipid (2.5%) and mineral (0.9%) proportions remained as a constant percentage of wet tissue weight during this period.

3.4 Kidneys and its Components

The earliest kidney structure to form is the pronephros and mesonephros around the fourth GW. At the fifth GW, the mesonephros provides a template for the adult metanephros. The critical window of kidney development spans 9–35 GW [58]. Kidney dimensions from ultrasound measurements have been reported from as early as 11 GW [59] and increase significantly during the second half of pregnancy owing to intense nephrogenesis and a significant increase in the number of nephrons [60].

The weight of both kidneys as a percentage of total body weight was found to be about 1.3% at 30 GW, 0.78% at birth, 0.58% by the age of 6 months and about 0.52% at 24 months [61]. Kidney volumes measured by ultrasound have been shown to be similar to those obtained via macrodissection ($p = 0.9$) [62]. Another study found that the calculation of kidney volume using an ellipsoid formula can underestimate the volume measured using a fluid displacement method by about 30% [63].

Studies reporting measurements of the mass of the kidneys are given in Table 4 of the ESM. A meta-analysis summary of these data at different FAs and body weights is given in Table 1. The following functions can be used to describe the total growth of both fetal kidneys during developments:

$$\begin{aligned} \text{Kidneys mass(g)} = & 0.1246 \cdot \text{FA} - 0.0333 \cdot \text{FA}^2 \\ & + 0.0026 \cdot \text{FA}^3 - 0.00003 \cdot \text{FA}^4 \end{aligned} \quad (13)$$

$$\text{Kidneys mass(g)} = 0.011 \cdot \text{BW} - 0.0000007 \cdot \text{BW}^2 \quad (14)$$

where FA is the fetal age in weeks and BW is the fetal body weight in grams. The provided polynomial age-based function was clearly superior to the power-type function described for previous organs (AIC: 60 vs. 129). Similarly, the polynomial weight-based function was superior to the linear and power models (AIC: 13, 53 and 34, respectively). Plots of data and best fit are given in Fig. 4 of the ESM. The kidney density is approximately 1.05 g/mL in fetuses aged 14–42 GW [47], 1.035 g/mL in the newborn and 1.05 g/mL in the adult [37].

The reported studies on the growth of the fetal renal cortex as well as medulla volumes are given in Table 5 of the ESM. These data show that the fastest growth of the renal cortex and medulla was found to be between 21 and 32 GW as a result of the increase in both the number and size of the glomeruli and the elongation of the cortical tortuous tubules [64, 65].

Collected data on fetal kidney tissue composition are limited to a few samples (Table 20 of the ESM) from two studies [42, 44]. The kidney water, as a percentage of wet tissue mass, decreases linearly with FA from the end of the first trimester till birth with an intercept of 94.227% and a negative FA coefficient of 0.2611. Both lipids and protein contents increase from 0.0 to 7.8% of the tissue weight at 14 GW to about 3.1 and 12% at term, while minerals remain constant during this period at about 0.8%.

Nephron formation begins at about 8 GW, by 20 GW about a third of the nephrons have been formed and, by 36 GW, adult numbers of nephrons are reached [66]. In pre-term infants born before 35 GW, nephron development continues until the infant reaches 35 post-conceptual weeks (see [48]). In a small sample of 22 observations from 11 fetuses (15–40 GW), the nephron volume was found to range from 0.00623 to 0.00857 mm³ with no significant change observed in the average volume of the whole nephron until 36 weeks [65]. Data on mean age-related changes in nephron volume, glomeruli number and size are shown in Table 5 of the ESM.

3.4.1 Glomerular Filtration Rate

The glomerulus is an unusual filtration barrier that retains higher molecular-weight proteins and blood cells in the circulation. Glomerular filtration begins before the end of the first trimester, when the first functional glomeruli appear. The glomerular filtration rate (GFR) shows a slow linear increase with age up to 34 GW, reflecting the development of nephrons and renal blood redistribution [67].

Fetal urinary flow rates have been used as a marker of fetal GFR because GFR increases with fetal weight and urine output increases with advancing gestation [68]. However, as in the postnatal kidney, urine output does not correlate well with absolute GFR. The glomerular number, which would also presumably reflect fetal kidney function, is also proportional to fetal weight. In fact, the increases in the glomerular number, GFR and fetal urine flow correlate closely with the increase in kidney mass, and it is therefore reasonable to assume that the main contributing factor is the addition of new nephrons [69, 70].

3.4.2 Urinary Bladder and Urine Production Rate

Fetal urinary bladder can be visualised by ultrasound from as early as 11 GW [59]. In a post-mortem study with detailed description of the bladder growth, the height, width and depth of the bladder was described in 149 foetuses [71] (Table 6 of the ESM). Bladder volume, based on two-dimensional ultrasonography from 11 dead foetuses, increases from 5.0 ± 0.87 to 10 ± 1.36, 20 ± 2.36, 30 ± 3.36 and 40 ± 4.36 mL at 20, 25, 35 and 40 GW, respectively [72].

Urine production starts between 10 and 12 GW [73]. Many studies quantified urine production rate using ultrasonography, but only data from three-dimensional (3D) ultrasonography studies (Table 6 of the ESM) were used for describing the fetal urine production rate, as two-dimensional ultrasonography cannot obtain both longitudinal and transverse images at the same time without a delay [74–76]. A meta-analysis of 3D studies shows that the average fetal urine production rate increased from 3.7 ± 2.1 mL (n = 6), 14.2 ± 7.0 mL (n = 21), 40.3 ± 23.1 mL (n = 27), 62.6 ± 28.7 mL (n = 22) and 87.1 ± 35.5 mL (n = 10) at 21, 25, 30, 35 and 38 weeks of FA, respectively (Fig. 5 of the ESM). The following equation can be used to describe the data between 20 and 38 weeks of FA:

$$\text{Urine production rate(ml/h)} = (0.081\text{FA})^{4.03}, \quad (15)$$

Water represents approximately 65% and minerals about 0.8% (0.5–1.1%) of the mass of the urinary bladder wall.

The urinary bladder contains about 0.02% of the total body blood in adults [22].

3.5 Pancreas

The fetal pancreas develops as early as 10 GW, and becomes vascularised by 16 GW [77, 78]. All pancreatic cell types are seen by 9–10 weeks [48].

Schulz et al. [185] examined the mass of the pancreas as a function of FA during the second half of pregnancy. Luecke et al. [20] recently expressed these data as a power function of the total body mass. Later, these data were extrapolation down to a FA of 8 weeks. Subsequently, Guihard-Costa et al. [118] and Phillips et al. [184] have reported the mass of the pancreas from the end of the first trimester until birth.

Collected data on the mass of the pancreas are given in Table 7 of the ESM. A meta-analysis of these data at different FAs and body weights are given in Table 1. Plots of growth of fetal pancreas as a function of FA and BW are given in Fig. 6 of the ESM. These summary measurements can be described using the following equations:

$$\text{Pancreas mass(g)} = (0.048 \cdot \text{FA})^{2.73}, \quad (16)$$

$$\text{Pancreas mass(g)} = (0.0018 \cdot \text{BW})^{0.91}. \quad (17)$$

where FA is the fetal age in weeks and BW is the fetal body weight in grams. No information on fetal pancreas density was found in the public domain. A value between 1.040 and 1.050 was reported for the adult pancreas [37].

Sex was not reported to be a significant covariate for the size of the fetal pancreas [79, 80]. Crown-rump length and GW were found to be significant covariates with regard to the pancreas length or width in 60 human foetuses of both sexes (28 female, 32 male) between the 17th and 40th week of intrauterine life [80].

No data could be found on fetal pancreas tissue composition. The adult pancreas is composed of about 71% water, 13% protein and 8% fat of the wet tissue weight [37].

3.6 Lungs

Fetal lungs begin to develop during early embryonic life, but can be identified using ultrasound from the age of 12 GW. Mucus production begins by 14 GW, while the terminal air sacs begin to appear between 24 and 26 GW [48], uniform alveolar structure are seen around 36 GW, but the majority of the alveoli develop after birth and increase in number until the age of 8 years [81]. Fetal lungs are inert and do not function as breathing organs. Nevertheless, by birth they must be developed to such an extent that they are immediately ready to function.

Studies reporting measurements of the mass of the lungs are given in Table 8 of the ESM. Meta-analysis of these studies at different FAs and body weights are given in Table 1. These summary measurements can be described using the following equations:

$$\text{Lungs mass(g)} = \frac{90.042 \cdot \text{FA}^{3.795}}{32.02^{3.795} + \text{FA}^{3.795}}, \quad (18)$$

$$\text{Lungs mass(g)} = 0.027 \cdot \text{BW} - 0.00000275 \cdot \text{BW}^2, \quad (19)$$

The provided age-based function was slightly superior to other functions (AIC were 103, 146 and 155 for sigmoidal, Weibull and power functions, respectively), while polynomial function predicted negative values for lung mass at an early FA. The polynomial weight-based function was superior to the other functions (AIC were 70.0, 75.7 and 75.8 for polynomial, Weibull and power function). Plots of growth of fetal lungs as a function of FA and body weight are given in Fig. 7 of the ESM. Comparison of mean lung (combined) volumes prior to autopsy to their weights at autopsy found a constant relationship during growth, with no significant deviation from linearity, in 25 foetuses aged 16–40 GW [51]. The density was found to be independent of GW between 9 and 20 GW [82] and found to be about 1.15 g/mL in 25 foetuses aged between 16 and 40 GW [51]. A value of 1.05 g/mL was reported for the foetus aged 14–42 GW [47] and a value of 0.90 g/mL was estimated for infant and children [47]. A value of 1.05 g/mL was reported for air-free adult lungs filled with blood [22]. Sex was not found to be a significant covariate for lung size [83].

Collected data on fetal lung tissue composition are limited to a few samples from two reports [40, 42], suggesting a relatively constant proportion of tissue composition during the second and third trimesters with 85.7% water, 2.0% lipid, 10.3% protein, 1.5% carbohydrates and 0.5% minerals.

3.7 Muscles

The intrauterine environment is a major determinant of the muscle mass that is present during the life course of an individual because muscle fibre number is set at the time of birth. The fibres are small, relatively few in number and widely separated by extracellular material between the fibres at 20 GW. At term, the fibres are still small, but there are many more of them and they are more closely packed together. In adult muscle, the fibres are very much larger in diameter and there is little space for extracellular material between the fibres [33]. The full complement of muscle cells is generally achieved by approximately 38 GW, with the formation of few new muscle cells after this time [4].

Fetal muscle was found to from about 14.3–18.5 and 20.5% of body weight at 16, 28 and 40 weeks of gestation [84]. In another study, fetal muscle mass was estimated from creatinine excretion rate in 31 male babies (25–34 GW, weighing 680–1830 g) during the first week of life and it was found that muscle mass increases from 12% of birth weight at 25 GW to 24% at 40 GW [85]. The study showed that birth weight and GW together accounted for 64% of the variance for muscle mass [85]. In two 6-month-old fetuses of 401 and 491 g body weight, the muscle mass was 22.75% [86]. The reference value for newborn infants is approximately 23% and increased to 40% for male adults and 29% for female adults [37].

Studies reporting measurement of the mass of the muscles are given in Table 9 of the ESM. A meta-analysis summary of these data at different FAs and body weights is given in Table 1. These summary measurements can be described using the following equations:

$$\text{Muscle mass(g)} = (0.194 \text{ FA})^{3.19}, \quad (20)$$

$$\text{Muscle mass(g)} = (0.029 \text{ BW})^{1.46}. \quad (21)$$

Plots of growth of fetal muscle as a function of FA and body weight are given in Fig. 8 of the ESM. No data could be found on fetal muscle density. Muscles density in adult is about 1.04 [37].

Available data on fetal skeletal muscle tissue composition were collected from five reports [31, 35, 42, 44, 87] and given in Table 20 of the ESM. These data suggest that total muscle water, percentage of tissue mass, decreases linearly with FA from the end of the first trimester till birth with an intercept of 94.696% and a negative FA coefficient of 0.2984. The extracellular water is about 77% of total muscle water at the start of the end of the first trimester and this decreases to 41.5% at term. This reduction in muscle water is associated with the accumulation of proteins from 7 to 17% and an increase in lipids from 0.9 to 2.0% between 13 and 38 weeks of FA. The phospholipid composition in fetal full-term ($n = 5$) skeletal muscles was reported to be about $2.5 \pm 0.5\%$ cardiolipin, $26.2 \pm 1.3\%$ ethanolamine phosphoglyceride, $45.9 \pm 2.3\%$ choline phosphoglyceride, $4.8 \pm 0.3\%$ inositol phosphoglyceride, $8.7 \pm 0.9\%$ serine phosphoglyceride and $11.8 \pm 0.9\%$ sphingomyelin of total phospholipids [87].

3.8 Spleen

The fetal spleen begins to form during the fifth week of embryonic development. The spleen is initially a haematopoietic organ and is a secondary site of red blood cell production until the fifth month of gestation, though after birth, red blood cells are only produced in the bone marrow. During the third trimester, spleen function

undergoes transition from a haematopoietic organ to acquire a definitive lymphoid character.

Studies reporting measurements of the mass of the spleen are given in Table 10 of the ESM. A meta-analysis of these data at different FAs and body weights is given in Table 1. These summary measurements can be described using the following equations:

$$\text{Spleen mass(g)} = (0.051 \cdot \text{FA})^{3.7}, \quad (22)$$

$$\text{Spleen mass(g)} = \frac{20.73 \cdot \text{BW}^{1.733}}{3054^{1.733} + \text{BW}^{1.733}}. \quad (23)$$

The provided age-based function (AIC = 65.3) was superior to the Weibull functions (AIC = 75.5), while polynomial function predicted negative values for spleen mass at an early FA (< 15 weeks). The weight-based sigmoidal function was superior to the other functions (AIC were -4.2 , 31.5 and 18.7 for sigmoidal, linear and power functions, respectively). Plots of growth of the fetal spleen as a function of FA and body weight are given in Fig. 9 of the ESM. The fetal spleen density is about 1.03 g/mL between 14 and 42 GW [47]. The adult value is approximately 1.06 g/mL [22].

Data on fetal spleen tissue composition are limited (see [42]), suggesting that constitutes of fetal spleen tissue are relatively constant between 24 and 38 weeks of FA. Their proportions as a percentage of the tissue are 83.8% water, 1.5% lipids, 13.9% protein and 0.8% minerals. The adult spleen is composed of about 77% water, 1.6% lipids and 18.8% protein of wet tissue [37].

3.9 Skin

Human skin undergoes marked structural and physiological changes during gestation. Human epidermal development undergoes four developmental stages; the embryonic period (< 9 GW), the stratification period (9–14 GW), follicular keratinisation (14–24 GW) and inter-follicular keratinisation (≥ 24 GW) [88]. All of the keratin proteins and filaggrin are present by 14–16 GW. At about 12 GW, hair follicles and associated glandular structure start to develop [88]. Sweat glands begin to appear by 14–16 GW, and are complete by 24 weeks [89]. Limited quantitative data are available on the growth of skin during fetal life [90, 91]. Usher and McLean measured abdominal skin thickness in millimetres, showing that the mean \pm SD (n) thickness increases from 2.34 ± 0.43 (13) to 4.51 ± 1.20 (13) and 5.41 ± 1.12 (47) at 25, 35 and 40 GW, respectively [91].

Collected data for skin weight (g) are limited mainly to those reported from 28 fetuses as part of a total dissection [90]. The original study also reported the change in the fetal hypodermis. About a 17.5-fold increase in absolute

skin weight has been reported between 21 GW and birth [92]. The reference values for skin and hypodermis weights of the newborn infant have been reported to be about 200 and 480 g, respectively [37]. These values are given in Table 11 of the ESM.

According to these data sets, the expected increases in fetal skin mass at different FAs and body weights are given in Table 1. The following equations can be used to describe the growth of fetal skin:

$$\text{Skin mass(g)} = (0.119 \cdot \text{FA})^{3.45}, \quad (24)$$

$$\text{Skin mass(g)} = 0.061 \cdot \text{BW}, \quad (25)$$

where FA is the fetal age in weeks and BW is the fetal body weight in grams. A plot of the growth of fetal skin is given in Fig. 10 of the ESM. The total skin density in most regions of the body is approximately 1.1 g/mL [22].

The expected values for hypodermis mass growth (g) are 0.003 ± 0.001 , 0.79 ± 0.66 , 47.2 ± 18.6 , 363.7 ± 113.2 and 529.9 ± 133.8 at 5, 15, 25, 35 and 38 weeks of FA, respectively. The growth of the hypodermis (g) can be predicted by the following equation:

$$\text{Hypodermis mass(g)} = 0.00004\text{BW}^2 + 0.0027\text{BW}. \quad (26)$$

A plot of the growth of fetal hypodermis is given in Fig. 11 of the ESM.

Quantitative data on skin composition during fetal life is limited to four reports [37, 42–44]. Fetal skin water decreases from 92% to 82.8% of fat-free skin between 11 and 38 weeks of FA. During this period, the fat-free skin protein increases from 7.4% to about 17%. The water content as a proportion of the whole skin was reported to be around 80% during fetal life and decreases to about 68% in full-term newborns [37].

3.10 Adipose

No quantitative measurement of total fetal adipose tissue could be found. The foetus is relatively lean during the first half of pregnancy, but thereafter fat starts to form and accumulates rapidly during the third trimester. We have reported the growth of total body fat in previous work [24]. Adipose tissue has a density of 0.92 g/mL [37]. Information on fetal adipose composition is limited to those reported for stillborn and newborn infants [42, 93, 94], suggesting 36% lipid, 6% protein and 57% water.

3.11 Bone

Fetal bones begin to develop at about 13 weeks following conception. From 25 GW to term, bone mineralisation increases by four-fold [48] reaching a value of

62.4 ± 18.3 g for the whole-body bone mineral content at full term [95] with about 32.1 ± 12.2 ($n = 20$), 39.5 ± 10.9 ($n = 76$) and 43.0 ± 11.7 g ($n = 20$) at 33, 34 and 36 GW, respectively, and its contribution to body weight remains relatively constant at about 1.7, 1.76 and 1.78% at these GW [96]. The bone mineral content was better correlated with birth weight rather than with GW [97]. Some studies focused on the growth of specific fetal bones such as the femoral [98–100], iliac [101] and limb [102].

Fetal dry and fat-free bone weights were reported for nine male and 11 female Caucasians, plus 12 male and 11 female black subjects between 21 and 43 GW [103]. Values of 420 g and 110 g have been quoted for fresh and dry bone mass at birth with a density of 1.08 g/mL [84]. The skeletal volume was reported for 16 foetuses between 29 and 41 GW using autopsy [104] and for 31 foetuses aged 14–41.5 GW assessed by a spiral computed tomography scanner [105].

Collected studies for the total bone are given in Table 12 of the ESM. Using the fetal-predicted body weight [24], the expected fetal bone mass at different FAs and body weights is given in Table 1. The following equations are proposed to predict total fetal bone:

$$\text{Bone weight (g)} = 0.0106 \text{FA}^3 - 0.2366 \text{FA}^2 + 3.2253 \text{FA}, \quad (27)$$

$$\text{Bone weight (g)} = 0.1035 \text{BW}. \quad (28)$$

When the dry fat-free skeletal weight of the human foetus is of interest, the following equation can be used:

$$\text{Dry fat-free skeletal weight} = 0.0294 \cdot \text{BW}. \quad (29)$$

A plot of fetal bone growth is given in Fig. 12 of the ESM. There are no clear data on bone density; however, this parameter is expected to be age dependent as a result of bone mineralisation. The density of the whole fresh adult skeleton is approximately 1.3 g/mL. Dry, mineralised collagenous bone matrix has a density of about 2.3 g/mL. The density of fresh bone that is free of marrow is typically 1.9–2.0 g/mL in the adult [22]. For newborns, cortical bone (g) constitutes about 36.5% of the total skeleton weight [37].

Collected data on fetal bone (femur bone and cartilages) tissue composition are available in Table 20 of the ESM from limited studies [32, 36, 38, 41, 42]. Femur water, percentage of tissue mass, decreases linearly with FA from the end of the first trimester till birth with an intercept of 84.926% and a negative FA coefficient of 0.6135. The extracellular water is about 44% of total bone water at the start of the second trimester and decreases up to 24% at term. This reduction in bone water is compensated by the accumulation of lipids, minerals and proteins.

3.12 Bone Marrow

Fetal mass of total bone marrow and that of the red marrow are essentially the same. This is because all fetal bone marrow is red except shortly before birth, when a small amount of fat may appear. Bone marrow volume from 16 fetuses (29–41 GW) with no skeletal abnormalities has been reported from post-mortem studies [104, 106]. Luecke et al [20] expressed these data as a power function of the total body mass with extrapolation for the whole fetal size. Similar extrapolation of this dataset was made by the International Commission on Radiological Protection [22] and derived “reference” values for the mass of fetal active marrow as a function of FA. Recently, Wilpshaar et al [107] reported bone marrow volumes from 12 fetuses during the second trimester using MRI techniques. Available data on bone marrow measurements are available in Table 13 of the ESM.

Analysis of the available data indicated that the expected fetal bone marrow volume (mL) increases from 0.008 ± 0.005 mL to 0.154 ± 0.070 , 1.23 ± 0.60 , 5.21 ± 0.87 , 13.8 ± 2.8 , 26.9 ± 5.1 , 42.3 ± 6.7 and 51.9 ± 6.7 mL at 5, 10, 15, 20, 25, 30, 35 and 38 weeks of FA, respectively. These summary measurements can be described using the following equations:

$$\text{Bone marrow(ml)} = \frac{\text{FA}^{6.45} \cdot 50.25}{\text{FA}^{6.45} + 30.0^{6.45}}, \quad (30)$$

$$\text{Bone marrow(ml)} = (0.011 \cdot \text{BW})^{1.073}, \quad (31)$$

where FA is the fetal age in weeks and BW is the fetal body weight in grams. Plot of growth fetal bone marrow volume is given in Fig. 13 of the ESM. There are no data on fetal bone marrow density, although Hudson suggested the value is close to 1.0 g/mL [104], whilst the International Commission on Radiological Protection mentioned a value of 1.028 g/mL [37].

3.13 Adrenal Glands

Adrenal glands can be identified as early as the 12th GW by ultrasonography [108], and can be recognised with fetal MRI, by 20 GW [109]. Throughout gestation, the size and weight of the fetal adrenal gland continuously grow. The relative adrenal gland size to body weight regresses substantially from the fetal value at birth during the neonatal period.

Studies reporting adrenal gland mass are given in Table 14 of the ESM. A meta-analysis of these data at different FAs and body weights is given in Table 1. These summary measurements can be described using the following equations:

$$\text{Adrenal gland mass(g)} = (0.063 \cdot \text{FA})^{2.38}, \quad (32)$$

$$\text{Adrenal gland mass(g)} = (0.0043 \cdot \text{BW})^{0.81}. \quad (33)$$

The provided age-based function was almost identical to the Weibull functions (AIC were 46.78 vs. 46.87), while polynomial function predicted negative values for adrenal gland mass at an early FA. The provided weight-based power function was superior to the polynomial, but identical to the Weibull functions (AIC were 6.46, 82.11 and 6.46). Plots of growth of fetal adrenal glands as a function of FA and body weight are given in Fig. 14 of the ESM. The adrenal gland density (g/mL) in a foetus aged 14–42 GW as about 0.87 [47] and in a male adult is approximately 1.02 [22].

No data could be found regarding fetal adrenal gland composition. In newborns, lipids constitute about 5% of the wet tissue weight, while water was found to constitute about 64% of the adrenal gland in a 14-year-old male individual [37].

3.14 Thymus

Differentiation of the thymus begins at 6–7 GW [4] and its size increases until birth after which the size, weight and activity of the gland decrease with age. Thymus dimensions (diameter and the perimeter) have been reported using ultrasonography for fetuses between 24 and 37 GW [110] and between 14 and 38 GW [111]. No correlation between thymus size and fetal sex was found between 16 and 37 GW [110, 112].

Collected studies reported the thymus gland mass are given in Table 15 of the ESM. A meta-analysis of these data at different FAs and body weights is given in Table 1. These summary measurements can be described using the following equations:

$$\text{Thymus gland mass(g)} = \frac{17.89 \cdot \text{FA}^{4.752}}{35.93^{4.752} + \text{FA}^{4.752}}, \quad (34)$$

$$\text{Thymus gland mass(g)} = \frac{17.89 \cdot \text{BW}^{1.587}}{2564^{1.587} + \text{BW}^{1.587}}. \quad (35)$$

The provided age-based sigmoidal function was superior to other functions (AIC were 38.9, 42.1 and 46.5 for sigmoidal, Weibull and power functions, respectively), while polynomial function predicted, inadequately, negative values for the organ mass at early FA. The weight-based sigmoidal function was superior to the power functions (AIC were -3.7 vs. 22.7). Plots of growth of the fetal thymus as a function of FA and body weight are given in Fig. 15 of the ESM. The thymus density is approximately 1.1 g/mL in fetuses aged 14–42 GW [47], 1.07 g/mL in the newborn and 1.025 g/mL in the adult [22].

No data could be found on fetal thymus tissue composition. About 82.2% of the adult thymus is water. In newborns, the thymus contains about 2.8% lipids (see [37]).

3.15 Thyroid Gland

The thyroid gland starts to develop by around the third week of intrauterine life. The functional activity begins by 12 GW [4]. After 20 GW, the thyroid gland undergoes progressive functional development towards term [113, 114]. The thyroid gland can be measured by ultrasonography from 14 GW [115]. Different studies have investigated the mass of the thyroid gland at different GW or body weight and using different methodologies [116–121]. The weight of the thyroid gland fixed in formalin has been reported to be similar to the freshly weighed specimens [122].

Data of thyroid gland mass are shown in Table 16 of the ESM. A meta-analysis of these data at different FAs and body weights is given in Table 1. These summary measurements can be described using the following equations:

$$\text{Thyroid mass(g)} = (0.033 \cdot \text{FA})^{2.585}, \quad (36)$$

$$\text{Thyroid mass(g)} = (0.00064 \cdot \text{BW})^{0.96}. \quad (37)$$

Plots of growth of the thyroid gland as a function of FA and body weight are given in Fig. 16 of the ESM. The thyroid gland density in an adult is approximately 1.05 g/mL [123].

Many system parameters were found positively correlated with fetal thyroid volume, such as GA, biparietal diameter, femur length, abdominal circumference and fetal weight [119, 124]. Sex is not a significant covariate [120, 122].

No data could be found for fetal thyroid composition. In adults, water constitutes about 72–78% of the gland, while protein constitutes about 14% of the wet weight of the gland [37].

3.16 Gastrointestinal Tract

The gut begins to appear during the fourth week as a tube and develops to the stage seen in the newborn by about 20 weeks [125]. Amniotic fluid swallowing activity has been observed around 16 weeks [126]. By 16 weeks, the foetus swallows 2–6 mL/day of amniotic fluid but this increases to 200–600 mL/day at term [48]. Villous formation begins at 7–8 GW and is present throughout the small intestine by 14 GW with well-developed crypts by about 19–20 GW [127–129]. Glucose and amino acids transports were found to be functional by around 18 GW [130, 131].

3.16.1 Stomach

The fetal stomach is sonographically visible at 9 GW and quantifiable after 10 GW [132]. It takes its final shape by 20–26 GW [133, 134]. Disputable attempts have been made to characterise the stomach volume growth using either ultrasonography [133, 135–137] or direct measurement of its weight [134]. Collated data are given in Table 17 of the ESM. These results are variable because of the complex structure of the stomach and its dynamically changing nature as a result of the filling with time, and use of different techniques.

Ultrasound measurements suggest that the volume of the stomach (mL) increased from 0.10 ± 0.04 to 0.32 ± 0.10 , 0.75 ± 0.58 , 2.12 ± 0.81 , 3.72 ± 1.94 , 5.12 ± 2.02 and 6.55 ± 1.44 at 12, 15, 18, 24, 30, 35 and 37 weeks of FA, respectively. These values can be described using the following equation:

$$\text{Gastric volume (mL)} = (0.053 \cdot \text{FA})^{2.73}. \quad (38)$$

A plot of the growth of the fetal stomach as a function of age is given in Fig. 17 of the ESM. No information could be found on the density of the fetal stomach. An adult stomach density is about 1.05 g/mL [138].

3.16.2 Intestines

Fetal intestinal length was measured at different GAS [139–143]. These data are given in Table 18 of the ESM. Age, weight and height, but not sex, were found to be significant covariates of intestinal length [142, 144]. Moderate/marked maceration was associated with colon length elongation, owing to the loss of smooth muscle tone, but none of the small intestine length, total bowel length or appendix length was altered by this [142]. Intrauterine growth restriction appears to affect fetal intestinal length during the third trimester, but no change could be detected during the second trimester [141, 142]. Down syndrome has been shown to influence the length of fetal intestines from the second trimester until birth [142, 143].

The length of the small intestine constitutes about 78, 82, 84.7 and 82.3% of the total length of the fetal intestines during the period of 11–12, 13–14, 19–20 and 23–24 GW, respectively [143]. Both the jejunum and the ileum constitute 97% of the small intestinal length, while the duodenum constitutes about 2–3% [139, 145]. The mean length of the small intestine, from necropsy measurements, shows an increase from 125 cm at 20 GW to 200 cm at 30 GW reaching 275 cm at term, indicating that fetal small intestinal growth exceeded that of body length [146]. Fetal colon length represents about 16.5, 18.8 and 16.2% of the overall length of the intestine at 19–27, 27–35 and > 35

GW, respectively [139], and its length increases by about two-fold during the third trimester [139].

3.16.3 Duodenum

Fetal duodenum dimensions were reported from a post-mortem study of 222 fetuses aged 9–40 GW with no external pathology or anomaly [144]. By assuming a cylinder shape and using the reported transverse diameter and length of the duodenum, the calculated volume shows an increase from 0.004 ± 0.001 mL to 0.12 ± 0.04 , 1.35 ± 0.27 and 3.35 ± 0.83 mL at 9, 22, 30 and 37 weeks of FA. The following equation can be used to describe these changes:

$$\text{Duodenal volume (mL)} = (0.053 \cdot \text{FA})^{2.73}. \quad (39)$$

3.16.4 Jejunum-ileum

The fetal jejunum-ileum length increases 2.4-fold compared with a 1.7-fold increase for the duodenum during the third trimester [139].

A detailed study measured jejunum and ileum diameters and their wall thickness throughout the fetal period in 131 subjects [147]. In adults, the jejunum constitutes about two-fifths of the small intestine [148]. Assuming this relationship is applicable for the fetal intestine, the calculated jejunum-ileum volume increased from 0.043 mL at 5 weeks of FA to 0.366, 3.12, 10.15 and 18.14 mL at 10, 20, 30 and 38 weeks of age, respectively. When these data were combined with the duodenal volume, the calculated overall length was similar to the direct measurements from post-mortem samples [149], as shown in Fig. 18 of the ESM. Thus, an equation based on these data sets can be derived to describe the growth of fetal small intestines as:

$$\text{Small intestine volume (mL)} = (0.061 \cdot \text{FA})^{3.905}. \quad (40)$$

Alternatively, a relationship can be derived to describe the small intestinal weight and body weight based on the direct measurement [149] as below:

$$\text{Fetal small intestine weight (gm)} = 0.0091 \cdot \text{BW}. \quad (41)$$

By propagating the variability in body weight, the expected variability in the fetal small intestine can be visualised in Fig. 18 of the ESM.

3.16.5 Colon

The weight of the fetal large intestine is less than that of small intestine [149] and can be distinguished from the small bowel by ultrasonography usually from 20 GW [150, 151]. It takes different shapes during fetal development reaching the adult form near term [152]. Collated studies for different dimensions of the fetal colon during

growth are given in Table 19 of the ESM, including colon diameter [152–157] and thickness [152].

The only data available for a normal fetal colon volume is from MRI for 83 measurements between 20 and 37 GW, showing that the fetal colon grows exponentially as a function of GW [158]. Correction for FA and extrapolation to the birth and zero at the FA of zero weeks yielded the following equation:

$$\text{Colon volume (ml)} = (0.060 \cdot \text{FA})^{4.98}. \quad (42)$$

The growth of the fetal colon can be visualised from Fig. 19 of the ESM.

3.16.6 Total Gut

Data on the total weight of the fetal gastrointestinal tract from Clatworthy and Anderson [159] show that the total alimentary canal weight increased from 0.3 g between 9 and 10 weeks of FA to 1.11, 8, 33, 85 and 100 g during 13–14, 19–20, 27–28, 35–36 and 37–38 weeks of FA, respectively. The reference value of 56 g for total newborn gastrointestinal tract weight was reported by the International Commission on Radiological Protection [160]. By combining stomach, small intestine and large intestine data, one can conclude that the weight of the total gastrointestinal tract increases from 0.038 g to 0.40, 1.83, 5.83, 14.9, 32.8, 65 and 94 g at 5, 10, 15, 20, 25, 30, 35 and 38 weeks of FA, respectively. These values are in agreement with those mentioned above from Clatworthy and Anderson (1944). The following equation can be used to describe the growth of the fetal gut:

$$\text{GI tract weight(g)} = (0.0737 \cdot \text{FA})^{4.41}. \quad (43)$$

Based on this function (Eq. 43) and the established age-weight relationship [24], the following function is suggested to describe the mass of the gut as a function of body weight:

$$\text{GI tract weight(g)} = 0.0081 \cdot \text{BW} + 0.000005 \cdot \text{BW}^2. \quad (44)$$

A plot of the growth of the fetal gut is given in Fig. 20 of the ESM.

No information on fetal stomach composition is available. The water constitutes about 75% of the adult stomach [37]. Fetal small intestines constitute about 2.2% water; of which 0.83 is phospholipids and 0.38% is cholesterol and about 0.10% is glycerides. These values are almost constant across different GAs [40]. A full-term intestines constitutes about 79% water, 2.5% lipids and 13% protein [37]. From seven premature newborns aged 28–33 GW, the

water content was found to be about 85.7% of the fat-free wet viscera tissue [35].

4 Discussion

This study summarises available data for the growth and composition of major fetal organs. The collated and integrated information has been analysed to derive growth parameters (point estimates and distributions) for organs during development, which are required to develop deterministic or stochastic PBPK models for this special population. The parameters are represented in terms of how they change from embryonic life to the end of gestation. This organ growth information together with previously reported information on fetal biometry and gross composition [24] when integrated within the PBPK model can offer an opportunity for assessing the fetal exposure and risk assessment to various xenobiotics at different stages of gestation.

To our knowledge, this is the first comprehensive source describing fetal organ growth data based on a meta-analysis with derived growth functions. Limited information is available from previous reviews [2, 17, 19, 161]. Among them, the most informative is the review by Archie et al., which includes the mean weight of nine fetal organs with the associated SDs at different GW; however, the data are only from autopsy studies and no growth functions were reported for these organs [17]. A recent pharmacokinetic-oriented study was performed to parametrise a linked fetal-maternal PBPK model. However, limited data were presented for only four organs using GA-dependent equations limited to 20–40 weeks in a deterministic manner, no attempt was made to conduct a meta-analysis or to quantify the inter-individual variability of fetal parameters [2].

Here, we take a different approach (i.e. stochastic), to build a bottom-up virtual population that considers inter-individual variability for each organ; first, by providing organ growth functions based on FA, with associated unlinked variability and, second, by facilitating a correlated Monte Carlo approach where links between organs and body weights are considered. The weight-based functions offer correlated variability, while the age-based functions do not. Where the age-dependent functions are used to build a fetal PBPK model, the variability terms (%CVs) in Table 1 are required to describe organ inter-individual variability.

The previously established male fetal body weight and its variability [24] was used in the current analysis in the following ways: (1) where no data on the body weight was reported for an organ, the established predicted mean values were used to map the body weight at each specific

reported FA to propose a relationship between the observed organ weight and total body weight as in the case of the gut; and (2) the established body weight variance was applied to the mean organ weight obtained by a meta-analysis to generate variability around the average values. The generated variability was compared to the observed variability of the organ and presented in the figures in the ESM.

In the previous study by Abduljalil et al. [24] the sample size for the fetal body weight was large and hence expected to follow a normal distribution; however, in the current study, limited data were found for few organs, especially for the very young foetuses, and the distribution may not follow the normal distribution. In the meta-analysis the normal distribution assumption was applied. From the provided figures (ESM), it appears the body weight variability adequately describes the variability in major organs such as the brain, heart and liver, but is not enough to describe small organs such as the adrenal glands and thymus. Possible reasons for this are that reported data for these organs were associated with high variability (CV was greater 40%) at certain ages or weights, different weight intervals reported in the original paper and/or non-standardised methodologies used to prepare and quantify the organ size.

While the growth of many normal fetal organs was described adequately, many challenges were encountered during data collection and analysis, which limited the effective use of available information. For example, some studies reported size measurements as a one-dimensional parameter such as the length or diameter [79, 162]. Such parameters are crude measures for characterising the growth of organs with a complex shape or with a dynamic state of filling and emptying as in the case of the gastrointestinal tract. Likewise, measurements of some organs were not reported, instead equations were reported for the mean with no information about the variability at different GW [163]. Such types of studies were excluded from the data analysis.

Another challenge was that many studies were cross-sectional and/or retrospective and some performed their analysis after pooling the data into monthly, trimester or multiple weekly intervals and reporting only the mean values. The selection of such intervals can introduce distortion in the results. In addition, many studies reported the results graphically and extracting the data from these figures may lead to technical errors.

For some parameters, such as volume or weight of the gut, skin and muscles, there were insufficient data to draw growth functions for these organs based on body weight. To overcome this challenge, the previously reported age-weight relationship was used to derive body weight-dependent equations for these organs.

Organs such as the thymus and adrenal glands are small and their measurements may not be reliable at early stages of gestation; however, they have been added to this article as there is accumulated evidence of drug toxicity to these organs from rodent and monkey species, but limited evidence so far from humans. For example, dexamethasone can depress fetal adrenal function [164]. Prenatal caffeine ingestion at a clinically toxic dose can inhibit fetal adrenal corticosterone production in rats [165]. Degenerative changes in fetal adrenal glands also have been reported after maternal nicotine exposure in rats [166]. Furthermore, there is evidence indicating that cadmium can accumulate in the fetal thymus [167]. Fetal thymic atrophy as a result of depression of the thymic cellularity and function has been reported after exposure to immunotoxicant compounds such as the insecticides chlordane and benzo(a)-pyrene [168, 169].

While the density of some fetal organs have been reported at certain points of development [51, 170], for other organs, densities are currently unavailable and thus reference values from newborns or adults were mentioned. A recent study showed that density did not differ between the lungs, kidneys, spleen, liver, adrenal glands and thymus evaluated, with advancing GW between 9 and 20 GW [82]. While it is possible, in this case, that below 20 GW no statistical difference in these organs density is expected, assuming the same value for each organ density after 20 GW is questionable. Future longitudinal studies are required to investigate the density of different organs at different FAs as such data are unavailable.

Tissue composition information is limited in general and reported mainly in older studies (see text). Where necessary, we used data from premature subjects to reflect in utero fetal composition at the equivalent age, as it is unlikely that there will be significant differences. However, longitudinal studies investigating tissue composition throughout in utero life using modern techniques are required.

Contradictory studies are reported on the accuracy of measurement techniques. Three studies have compared autopsy weight vs. MRI volume on post-mortem fetal organ measurement. In Breeze et al., fetal lung, brain and liver volumes were estimated post-mortem in a total of 25 fetuses at 16–40 GW and showed a good correlation between volume estimated at MRI and weight estimated at post-mortem [51]. Thayyil et al. examined fetal liver, spleen, adrenal glands, thymus, heart, kidneys and lungs in a total of 30 fetuses at 14–42 GW and showed a high linear correlation between estimated and actual weights. It also showed that accuracy was lower when fetuses were < 20 GW or < 300 g in weight. The weight of the organs measured varied between 6 and 161 g [170]. Votino et al. examined fetal liver, lungs, kidneys, adrenal glands,

thymus and spleen, but focusing on smaller fetuses, 9–20 GW, and thus on smaller organs (0.009–6 g) [82]. In this study, the volume and weight for all investigated organs were linearly correlated in a statistically significant manner.

Magnetic resonance imaging was found to overestimate the fetal autopsy lung volume between 9 and 19 GW by a mean of 138 mm³ [82]. Magnetic resonance imaging tends to slightly overestimate the average volume of some organs such as the liver, lungs and brain most probably owing to fluid loss or lack of perfusion at the time of autopsy. However, when the autopsy studies are compiled together, the MRI measurements are within the inter-autopsy study variability. Therefore, values from MRI were included in the data analysis without special treatment. The two-dimensional ultrasound method was found to overestimate all lung volumes in relation to those obtained by virtual organ computer-aided analysis (VOCAL) [171]. The 3D ultrasound produces slightly lower lung volume when compared with MRI [172]. The VOCAL 3D-ultrasound measurements of lungs showed higher variability than those obtained by means of MRI [173] and overestimate autopsy measurements, as in the case of the heart data. The extended version of VOCAL (XI VOCAL) has been developed [174] and reported to accurately virtualise actual organs by analysing the volume of the organs drawn out from a sliced sectional diagram. The XI VOCAL is reported to be better than VOCAL and 3D ultrasonography in the measurement of the volume of organs with irregular shapes [174, 175] and provided more accurate measurements than VOCAL for fetal heart volume [175]. With increased interest in the new techniques, longitudinal studies using standard methods with an accurate determination of organs are required. Unfortunately, there is not yet a comprehensive review of the accuracy of these methods during the entire intra-uterine fetal period.

Despite all the challenges described above, the current level of data collection on fetal organ seems sufficient as a starting point for building fetal PBPK models, encompassing longitudinal changes of anatomical values with FA and or body weight. The fetal organ growth data alongside previous fetal biometry data and future data on fetal organ blood flows, blood binding parameters, drug metabolism and transporter ontogeny will allow complete parametrisation of a full fetal PBPK model. Integration of fetal physiological parameters with maternal physiological parameters, together with the placental unit within the PBPK platform will facilitate assessment of inadvertent fetal exposure to drugs and xenobiotics after maternal administration and in clinical settings when the foetus is the therapeutic target. Compiled fetal PBPK models will require verification of their performance against field data (clinical observation on pharmaceutical drugs or

opportunistic data on environmental chemicals). Such models have to be viewed as “live models”, which are built on a flexible framework that allow new data to be incorporated as they become available. To develop a mechanistic PBPK model, a multivariate analysis of maternal and fetal covariates, their means and distributions should be performed and the results integrated within the PBPK platform.

The current evaluation of these data was carried out based on the collected data presented in the tables in the ESM. Thus, the provided mean and variability values for poorly described parameters may not represent the actual mean or variability in a real-life situation.

5 Conclusions

This is the first work to provide a comprehensive data collection for fetal organs from numerous scattered studies and to analyse them and propose an analytical solution describing organ growth with age and body weight. These tasks were undertaken primarily to fill some of the existing gaps in our knowledge regarding this special population and thus enable the construction of mechanistic fetal PBPK models that can be linked to a maternal model and used to predict fetal exposure and potential toxicity. While the current article provides an up-to-date database, it also identifies gaps in existing knowledge and areas where further research is required.

Acknowledgements We thank Miss Eleanor Savill and Ms Rosalie Bower for their assistance with collecting the references and preparing the manuscript.

Compliance with Ethical Standards

Funding No funding was received for the preparation of this study.

Conflict of interest Khaled Abduljalil, Masoud Jamei and Trevor N. Johnson are full-time employees of Certara UK Limited. The activities of Certara are supported by a consortium of pharmaceutical companies.

References

- Zhang Z, Unadkat JD. Development of a novel maternal-fetal physiologically based pharmacokinetic model II: verification of the model for passive placental permeability drugs. *Drug Metab Dispos.* 2017;45:939–46.
- Zhang Z, Imperial MZ, Patilea-Vrana GI, Wedagedera J, Gao-hua L, Unadkat JD. Development of a novel maternal-fetal physiologically based pharmacokinetic model I: insights into factors that determine fetal drug exposure through simulations and sensitivity analyses. *Drug Metab Dispos.* 2017;45:920–38.
- O’Rahilly R, Muller F. Developmental stages in human embryos: revised and new measurements. *Cells Tissues Organs.* 2010;192:73–84.
- Moore KL, Persaud TVN, Torchia MG. The developing human: clinically oriented embryology. 9th ed. Philadelphia (PA): Saunders, Elsevier; 2013.
- Sachdeva P, Patel BG, Patel BK. Drug use in pregnancy; a point to ponder! *Indian J Pharm Sci.* 2009;71:1–7.
- Colbers A, Greupink R, Burger D. Pharmacological considerations on the use of antiretrovirals in pregnancy. *Curr Opin Infect Dis.* 2013;26:575–88.
- Cox PB, Marcus MA, Bos H. Pharmacological considerations during pregnancy. *Curr Opin Anaesthesiol.* 2001;14:311–6.
- Herbst AL, Ulfelder H, Poskanzer DC. Adenocarcinoma of the vagina: association of maternal stilbestrol therapy with tumor appearance in young women. *N Engl J Med.* 1971;284:878–81.
- Edelman DA. Diethylstilbestrol exposure and the risk of clear cell cervical and vaginal adenocarcinoma. *Int J Fertil.* 1989;34:251–5.
- Drukker A, Guignard JP. Renal aspects of the term and preterm infant: a selective update. *Curr Opin Pediatr.* 2002;14:175–82.
- Brenner BM, Chertow GM. Congenital oligonephropathy and the etiology of adult hypertension and progressive renal injury. *Am J Kidney Dis.* 1994;23:171–5.
- Poggi SH, Ghidini A. Importance of timing of gestational exposure to methotrexate for its teratogenic effects when used in setting of misdiagnosis of ectopic pregnancy. *Fertil Steril.* 2011;96:669–71.
- Sulik KK, Cook CS, Webster WS. Teratogens and craniofacial malformations: relationships to cell death. *Development.* 1988;103 Suppl.:213–31.
- Martin-Suarez A, Sanchez-Hernandez JG, Medina-Barajas F, Perez-Blanco JS, Lanao JM, Garcia-Cuenillas Alvarez L, et al. Pharmacokinetics and dosing requirements of digoxin in pregnant women treated for fetal supraventricular tachycardia. *Expert Rev Clin Pharmacol.* 2017;10:911–7.
- Roberts D, Brown J, Medley N, Dalziel SR. Antenatal corticosteroids for accelerating fetal lung maturation for women at risk of preterm birth. *Cochrane Database Syst Rev.* 2017;3:CD004454.
- Miyata I, Abe-Gotyo N, Tajima A, Yoshikawa H, Teramoto S, Seo M, et al. Successful intrauterine therapy for fetal goitrous hypothyroidism during late gestation. *Endocr J.* 2007;54:813–7.
- Archie JG, Collins JS, Lebel RR. Quantitative standards for fetal and neonatal autopsy. *Am J Clin Pathol.* 2006;126:256–65.
- Shepard TH, Shi M, Fellingham GW, Fujinaga M, FitzSimmons JM, Fantel AG, et al. Organ weight standards for human fetuses. *Pediatr Pathol.* 1988;8:513–24.
- Jackson CM. On the prenatal growth of the human body and the relative growth of the various organs and parts. *Am J Anat.* 1909;9:119–65.
- Luecke RH, Wosilait WD, Young JF. Mathematical representation of organ growth in the human embryo/fetus. *Int J Biomed Comput.* 1995;39:337–47.
- Potter EL, Craig JM. Potter’s pathology of the fetus and infant. St. Louis (MO): Mosby; 1997.
- Valentin J. Basic anatomical and physiological data for use in radiological protection: reference values: a report of age- and gender-related differences in the anatomical and physiological characteristics of reference individuals. ICRP Publication 89. *Ann ICRP.* 2002;32:5–265.
- Abduljalil K, Furness P, Johnson TN, Rostami-Hodjegan A, Soltani H. Anatomical, physiological and metabolic changes with gestational age during normal pregnancy: a database for parameters required in physiologically based pharmacokinetic modelling. *Clin Pharmacokinet.* 2012;51:365–96.

24. Abduljalil K, Johnson NT, Rostami-Hodjegan A. Fetal physiologically-based pharmacokinetic models: systems information on fetal biometry and gross composition. *Clin Pharmacokinet* (accepted).
25. Silverwood RJ, Cole TJ. Statistical methods for constructing gestational age-related reference intervals and centile charts for fetal size. *Ultrasound Obstet Gynecol.* 2007;29:6–13.
26. Tanimura T, Nelson T, Hollingsworth RR, Shepard TH. Weight standards for organs from early human fetuses. *Anat Rec.* 1971;171:227–36.
27. Marecki B. Sexual dimorphism of the weight of internal organs in fetal ontogenesis. *Anthropol Anz.* 1989;47:175–84.
28. Fujikura T, Froehlich LA. Organ-weight-brain-weight ratios as a parameter of prenatal growth: a balanced growth theory of viscera. *Am J Obstet Gynecol.* 1972;112:896–902.
29. Burdi AR, Barr M, Babler WJ. Organ weight patterns in human fetal development. *Hum Biol.* 1981;53:355–66.
30. Baker GL. Human adipose tissue composition and age. *Am J Clin Nutr.* 1969;22:829–35.
31. Brans YW, Shannon DL. Chemical changes in human skeletal muscle during fetal development. *Biol Neonate.* 1981;40:21–8.
32. Dickerson JW. Changes in the composition of the human femur during growth. *Biochem J.* 1962;82:56–61.
33. Dickerson JW, Widdowson EM. Chemical changes in skeletal muscle during development. *Biochem J.* 1960;74:247–57.
34. Dobbing J, Sands J. Quantitative growth and development of human brain. *Arch Dis Child.* 1973;48:757–67.
35. Fee BA, Weil WB Jr. Body composition of infants of diabetic mothers by direct analysis. *Ann N Y Acad Sci.* 1963;110:869–97.
36. Fomon SJ, Haschke F, Ziegler EE, Nelson SE. Body composition of reference children from birth to age 10 years. *Am J Clin Nutr.* 1982;35:1169–75.
37. ICRP. Report of the Task Group on Reference Man. ICRP Publication 23, International Commission on Radiological Protection. Oxford: Pergamon Press; 1975.
38. Iob V, Swanson WW. The extracellular and intracellular water in bone and cartilage. *J Biol Chem.* 1938;122:485–90.
39. Iyengar L, Apte SV. Nutrient stores in human foetal livers. *Br J Nutr.* 1972;27:313–7.
40. Shah RS, Rajalakshmi R. Studies on human fetal tissues: II. Lipid composition of human fetal tissues in relation to gestational age, fetal size and maternal nutritional status. *Indian J Pediatr.* 1988;55:272–82.
41. Swanson WW, IOB V. Growth and chemical composition of the human skeleton. *Am J Dis Child.* 1940;59:107–11.
42. White DR, Widdowson EM, Woodard HQ, Dickerson JW. The composition of body tissues (II): fetus to young adult. *Br J Radiol.* 1991;64:149–59.
43. Widdowson EM. Growth and composition of the fetus and newborn. In: Assali NS, editor. *Biology of gestation.* Vol 2. The fetus and neonate. New York (NY): Academic Press; 1968. p. 1–49.
44. Widdowson EM, Dickerson JW. The effect of growth and function on the chemical composition of soft tissues. *Biochem J.* 1960;77:30–43.
45. Winick M. Changes in nucleic acid and protein content of the human brain during growth. *Pediatr Res.* 1968;2:352–5.
46. Valenti O, Di Prima FA, Renda E, Faraci M, Hyseni E, De Domenico R, et al. Fetal cardiac function during the first trimester of pregnancy. *J Prenat Med.* 2011;5:59–62.
47. Thayyil S, Schievano S, Robertson NJ, Jones R, Chitty LS, Sebire NJ, et al. A semi-automated method for non-invasive internal organ weight estimation by post-mortem magnetic resonance imaging in fetuses, newborns and children. *Eur J Radiol.* 2009;72:321–6.
48. Blackburn ST. *Maternal, fetal and neonatal physiology: a clinical perspective.* 3rd ed. Philadelphia: Saunders Elsevier; 2007.
49. Khwaja OS, Pomeroy SL, Ullrich NJ. Development of the nervous system. In: Polin RA, Fox WW, Abman SH, editors. *Fetal and neonatal physiology.* 4th ed. Philadelphia (PA): Elsevier; 2011. p. 1745–62.
50. Samuelsen GB, Larsen KB, Bogdanovic N, Laursen H, Graem N, Larsen JF, et al. The changing number of cells in the human fetal forebrain and its subdivisions: a stereological analysis. *Cereb Cortex.* 2003;13:115–22.
51. Breeze AC, Gallagher FA, Lomas DJ, Smith GC, Lees CC. Postmortem fetal organ volumetry using magnetic resonance imaging and comparison to organ weights at conventional autopsy. *Ultrasound Obstet Gynecol.* 2008;31:187–93.
52. Duck FA. *Physical properties of tissue.* London: Academic; 1990.
53. Johansson M, Strahm E, Rane A, Ekstrom L. CYP2C8 and CYP2C9 mRNA expression profile in the human fetus. *Front Genet.* 2014;5:58.
54. Fanni D, Fanos V, Ambu R, Lai F, Gerosa C, Pampaloni P, et al. Overlapping between CYP3A4 and CYP3A7 expression in the fetal human liver during development. *J Matern Fetal Neonatal Med.* 2014;1–5.
55. Hakkola J, Raunio H, Purkunen R, Saarikoski S, Vahakangas K, Pelkonen O, et al. Cytochrome P450 3A expression in the human fetal liver: evidence that CYP3A5 is expressed in only a limited number of fetal livers. *Biol Neonate.* 2001;80:193–201.
56. Hakkola J, Pasanen M, Purkunen R, Saarikoski S, Pelkonen O, Maenpaa J, et al. Expression of xenobiotic-metabolizing cytochrome P450 forms in human adult and fetal liver. *Biochem Pharmacol.* 1994;48:59–64.
57. Hines RN. The ontogeny of drug metabolism enzymes and implications for adverse drug events. *Pharmacol Ther.* 2008;118:250–67.
58. Gasser B, Mauss Y, Ghnassia JP, Favre R, Kohler M, Yu O, et al. A quantitative study of normal nephrogenesis in the human fetus: its implication in the natural history of kidney changes due to low obstructive uropathies. *Fetal Diagn Ther.* 1993;8:371–84.
59. Rosati P, Guariglia L. Transvaginal sonographic assessment of the fetal urinary tract in early pregnancy. *Ultrasound Obstet Gynecol.* 1996;7:95–100.
60. Vlajković S, Daković-Bjelaković M, Čukuranović R, Krivokuća D. The average volume of fetal kidney during different periods of gestation. *Acta Medica Medianae.* 2005;44:47–50.
61. Geelhoed JJ, Taal HR, Steegers EA, Arends LR, Lequin M, Moll HA, et al. Kidney growth curves in healthy children from the third trimester of pregnancy until the age of two years: the Generation R Study. *Pediatr Nephrol.* 2010;25:289–98.
62. Jovevska S, Tofoski G. Comparison between ultrasound (US) and macrodissection measurements of human foetal kidney. *Prilozi.* 2008;29:337–44.
63. Vlajkovic S, Vasovic L, Dakovic-Bjelakovic M, Cukuranovic R. Age-related changes of the human fetal kidney size. *Cells Tissues Organs.* 2006;182:193–200.
64. Vlajkovic S, Dakovic-Bjelakovic M, Cukuranovic R, Popovic J. Evaluation of absolute volume of human fetal kidney's cortex and medulla during gestation. *Vojnosanit Pregl.* 2005;62:107–11.
65. Hinchliffe SA, Sargent PH, Howard CV, Chan YF, van Velzen D. Human intrauterine renal growth expressed in absolute number of glomeruli assessed by the disector method and Cavalieri principle. *Lab Invest.* 1991;64:777–84.
66. Haycock GB. Development of glomerular filtration and tubular sodium reabsorption in the human fetus and newborn. *Br J Urol.* 1998;81(Suppl. 2):33–8.

67. Seikaly MG, Arant BS Jr. Development of renal hemodynamics: glomerular filtration and renal blood flow. *Clin Perinatol.* 1992;19:1–13.
68. Rabinowitz R, Peters MT, Vyas S, Campbell S, Nicolaidis KH. Measurement of fetal urine production in normal pregnancy by real-time ultrasonography. *Am J Obstet Gynecol.* 1989;161:1264–6.
69. Manalich R, Reyes L, Herrera M, Melendi C, Fundora I. Relationship between weight at birth and the number and size of renal glomeruli in humans: a histomorphometric study. *Kidney Int.* 2000;58:770–3.
70. Trnka P, Hiatt MJ, Tarantal AF, Matsell DG. Congenital urinary tract obstruction: defining markers of developmental kidney injury. *Pediatr Res.* 2012;72:446–54.
71. Sulak O, Cankara N, Malas MA, Koyuncu E, Desdicioglu K. Anatomical development of urinary bladder during the fetal period. *Clin Anat.* 2008;21:683–90.
72. Hedriana HL, Moore TR. Ultrasonographic evaluation of human fetal urinary flow rate: accuracy limits of bladder volume estimations. *Am J Obstet Gynecol.* 1994;170:1250–4.
73. Woolf AS. Perspectives on human perinatal renal tract disease. *Semin Fetal Neonatal Med.* 2008;13:196–201.
74. Lee SM, Park SK, Shim SS, Jun JK, Park JS, Syn HC. Measurement of fetal urine production by three-dimensional ultrasonography in normal pregnancy. *Ultrasound Obstet Gynecol.* 2007;30:281–6.
75. Maged AM, Abdelmoneim A, Said W, Mostafa WA. Measuring the rate of fetal urine production using three-dimensional ultrasound during normal pregnancy and pregnancy-associated diabetes. *J Matern Fetal Neonatal Med.* 2014;27(17):1790–4.
76. Touboul C, Boulvain M, Picone O, Levaillant JM, Frydman R, Senat MV. Normal fetal urine production rate estimated with 3-dimensional ultrasonography using the rotational technique (virtual organ computer-aided analysis). *Am J Obstet Gynecol.* 2008;199(1):57.e1–5.
77. Bouwens L, Lu WG, De Krijger R. Proliferation and differentiation in the human fetal endocrine pancreas. *Diabetologia.* 1997;40:398–404.
78. Robb P. The development of the islets of Langerhans in the human foetus. *Q J Exp Physiol Cogn Med Sci.* 1961;46:335–43.
79. Desdicioglu K, Malas MA, Evcil EH. Foetal development of the pancreas. *Folia Morphol (Warsz).* 2010;69:216–24.
80. Krakowiak-Sarnowska E, Flisinski P, Szpinda M, Sarnowski J, Lisewski P, Flisinski M. Morphometry of the pancreas in human foetuses. *Folia Morphol (Warsz).* 2005;64:29–32.
81. Langston C, Kida K, Reed M, Thurlbeck WM. Human lung growth in late gestation and in the neonate. *Am Rev Respir Dis.* 1984;129:607–13.
82. Votino C, Verhoye M, Segers V, Cannie M, Bessieres B, Cos T, et al. Fetal organ weight estimation by postmortem high-field magnetic resonance imaging before 20 weeks' gestation. *Ultrasound Obstet Gynecol.* 2012;39:673–8.
83. Ishak N, Sozo F, Harding R, De Matteo R. Does lung development differ in male and female fetuses? *Exp Lung Res.* 2014;40:30–9.
84. Blackfan KD. Growth and development of the child. Part II: anatomy and physiology. Report of the Committee on Growth and Development. New York (NY): The Century Company; 1933.
85. Modi N, Hutton JL. Urinary creatinine excretion and estimation of muscle mass in infants of 25–34 weeks gestation. *Acta Paediatr Scand.* 1990;79:1156–62.
86. Malina RM. Growth of muscle tissue and muscle mass. In: Falkner F, Tanner JM, editors. *Human growth: a comprehensive treatise.* 2nd ed. New York (NY): Plenum Press; 1986. p. 77–99.
87. Bruce A. Skeletal muscle lipids. II. Changes in phospholipid composition in man from fetal to middle age. *J Lipid Res.* 1974;15:103–8.
88. Dale BA, Holbrook KA, Kimball JR, Hoff M, Sun TT. Expression of epidermal keratins and filaggrin during human fetal skin development. *J Cell Biol.* 1985;101:1257–69.
89. Li J, Fu X, Sun X, Sun T, Sheng Z. The interaction between epidermal growth factor and matrix metalloproteinases induces the development of sweat glands in human fetal skin. *J Surg Res.* 2002;106:258–63.
90. Roe HE. The weight of the skin and tela subcutanea of the human fetus. *Anat Rec.* 1933;55:127–37.
91. Usher R, McLean F. Intrauterine growth of live-born Caucasian infants at sea level: standards obtained from measurements in 7 dimensions of infants born between 25 and 44 weeks of gestation. *J Pediatr.* 1969;74:901–10.
92. Wilmer HA. Quantitative growth of skin and subcutaneous tissue in relation to human surface area. *Proc Soc Exp Biol Med.* 1940;43:386–8.
93. Baker PN, Johnson IR, Gowland PA, Hykin J, Harvey PR, Freeman A, et al. Fetal weight estimation by echo-planar magnetic resonance imaging. *Lancet.* 1994;343:644–5.
94. Friis-Hansen B. Body composition during growth: in vivo measurements and biochemical data correlated to differential anatomical growth. *Pediatrics.* 1971;47:Suppl. 2:264.
95. Lapillonne AA, Glorieux FH, Salle BL, Braillon PM, Chambon M, Rigo J, et al. Mineral balance and whole body bone mineral content in very low-birth-weight infants. *Acta Paediatr.* 1994;405:117–22.
96. Demarini S, Koo WW, Hockman EM. Bone, lean and fat mass of newborn twins versus singletons. *Acta Paediatr.* 2006;95:594–9.
97. Lapillonne A, Braillon P, Claris O, Chatelain PG, Delmas PD, Salle BL. Body composition in appropriate and in small for gestational age infants. *Acta Paediatr.* 1997;86:196–200.
98. Salle BL, Rauch F, Travers R, Bouvier R, Glorieux FH. Human fetal bone development: histomorphometric evaluation of the proximal femoral metaphysis. *Bone.* 2002;30:823–8.
99. Harvey NC, Mahon PA, Robinson SM, Nisbet CE, Javadi MK, Crozier SR, et al. Different indices of fetal growth predict bone size and volumetric density at 4 years of age. *J Bone Miner Res.* 2010;25:920–7.
100. Walsh JM, Kilbane M, McGowan CA, McKenna MJ, McAuliffe FM. Pregnancy in dark winters: implications for fetal bone growth? *Fertil Steril.* 2013;99:206–11.
101. Kara SA, Toppare MF. Ultrasonographic dimensions of the vertical span of the fetal iliac bone and relationship with some fetal parameters. *Prenatal Diagn.* 1998;18:127–32.
102. Scheuer JL, Musgrave JH, Evans SP. The estimation of late fetal and perinatal age from limb bone length by linear and logarithmic regression. *Ann Hum Biol.* 1980;7:257–65.
103. Trotter M, Peterson RR. Weight of bone in the fetus during the last half of pregnancy. *Clin Orthop Relat Res.* 1969;65:46–50.
104. Hudson G. Bone-marrow volume in the human foetus and newborn. *Br J Haematol.* 1965;11:446–52.
105. Braillon PM, Buenerd A, Lapillonne A, Bouvier R. Skeletal and total body volumes of human fetuses: assessment of reference data by spiral CT. *Pediatr Radiol.* 2002;32:354–9.
106. Hudson G. Organ size of human foetal bone marrow. *Nature.* 1965;205:96–7.
107. Wilpshaar J, Joeke EC, Lim FT, Van Leeuwen GA, Van den Boogaard PJ, Kanhai HH, et al. Magnetic resonance imaging of fetal bone marrow for quantitative definition of the human fetal stem cell compartment. *Blood.* 2002;100:451–7.
108. Bronshtein M, Tzidony D, Dimant M, Hajos J, Jaeger M, Blumenfeld Z. Transvaginal ultrasonographic measurements of the

- fetal adrenal glands at 12 to 17 weeks of gestation. *Am J Obstet Gynecol.* 1993;169:1205–10.
109. Brugger PC, Prayer D. Fetal abdominal magnetic resonance imaging. *Eur J Radiol.* 2006;57:278–93.
 110. De Leon-Luis J, Gamez F, Pintado P, Antolin E, Perez R, Ortiz-Quintana L, et al. Sonographic measurements of the thymus in male and female fetuses. *J Ultrasound Med.* 2009;28:43–8.
 111. Zalel Y, Gamzu R, Mashiach S, Achiron R. The development of the fetal thymus: an in utero sonographic evaluation. *Prenat Diagn.* 2002;22:114–7.
 112. Liberti EA, Villa N, Melhem SA, Matson E, Konig B Jr, Adamo J. A morphometrical study of human fetal thymus. *Z Mikrosk Anat Forsch.* 1989;103:309–15.
 113. Patel J, Landers K, Li H, Mortimer RH, Richard K. Thyroid hormones and fetal neurological development. *J Endocrinol.* 2011;209:1–8.
 114. Hobel CJ. Fetal thyroid. *Clin Obstet Gynecol.* 1980;23:779–90.
 115. Cohen O, Pinhas-Hamiel O, Sivan E, Dolitski M, Lipitz S, Achiron R. Serial in utero ultrasonographic measurements of the fetal thyroid: a new complementary tool in the management of maternal hyperthyroidism in pregnancy. *Prenat Diagn.* 2003;23:740–2.
 116. Ares S, Pastor I, Quero J, Morreale de Escobar G. Thyroid gland volume as measured by ultrasonography in preterm infants. *Acta Paediatr.* 1995;84:58–62.
 117. Bocian-Sobkowska J, Wozniak W, Malendowicz LK. Morphometric studies on the development of the human thyroid gland. II. The late fetal life. *Histol Histopathol.* 1997;12:79–84.
 118. Guihard-Costa AM, Menez F, Delezoide AL. Organ weights in human fetuses after formalin fixation: standards by gestational age and body weight. *Pediatr Dev Pathol.* 2002;5:559–78.
 119. Ho SS, Metreweli C. Normal fetal thyroid volume. *Ultrasound Obstet Gynecol.* 1998;11:118–22.
 120. Ozguner G, Sulak O. Size and location of thyroid gland in the fetal period. *Surg Radiol Anat.* 2014;36:359–67.
 121. Savin-Žegarac S, Cvejic D, Nedić O, Radosavljević R, Ivana MP. Iodine and iodothyronine content in human neonate thyroid gland. *Arch Biol Sci.* 2002;54(3–4):69–74.
 122. Shepard TH, Andersen HJ, Andersen H. The human fetal thyroid. I. Its weight in relation to body weight, crown-rump length, foot length and estimated gestation age. *Anat Rec.* 1964;148:123–8.
 123. Valentin J. Basic anatomical and physiological data for use in radiological protection: reference values: ICRP Publication 89. *Ann ICRP.* 2002;32:1–277.
 124. Seely BL, Burrow GN. Thyroid disease and pregnancy. In: Creasy RK, Resnik R, editors. *Maternal fetal medicine: principle and practice.* Philadelphia (PA): WB Saunders; 1994. p. 979–1001.
 125. Weaver LT. Anatomy and embryology. In: Walker WA, Dune PR, Hamilton RJ, editors. *Pediatric gastrointestinal disease.* 2nd ed. St. Louis (MO): Mosby; 1996.
 126. Pritchard JA. Fetal swallowing and amniotic fluid volume. *Obstet Gynecol.* 1966;28:606–10.
 127. Menard D. Functional development of the human gastrointestinal tract: hormone- and growth factor-mediated regulatory mechanisms. *Can J Gastroenterol.* 2004;18:39–44.
 128. Grand RJ, Watkins JB, Torti FM. Development of the human gastrointestinal tract: a review. *Gastroenterology.* 1976;70:790–810.
 129. Bates MD, Balistreri WF. The gastrointestinal tract: development of the human digestive system. In: Fanaroff AA, Martin RJ, editors. *Neonatal-perinatal medicine: diseases of the fetus and infant.* 7th ed. St. Louis (MO): Mosby; 2002.
 130. Malo C. Multiple pathways for amino acid transport in brush border membrane vesicles isolated from the human fetal small intestine. *Gastroenterology.* 1991;100:1644–52.
 131. Lebenthal A, Lebenthal E. The ontogeny of the small intestinal epithelium. *JPEN J Parenter Enteral Nutr.* 1999;23(5 Suppl.):S3–6.
 132. Goldstein I, Reece EA, Yarkoni S, Wan M, Green JL, Hobbins JC. Growth of the fetal stomach in normal pregnancies. *Obstet Gynecol.* 1987;70:641–4.
 133. Nagata S, Koyanagi T, Fukushima S, Akazawa K, Nakano H. Change in the three-dimensional shape of the stomach in the developing human fetus. *Early Hum Dev.* 1994;37:27–38.
 134. Gworys B, Jeka S, Brukiewa R, Rymko M. Dynamics of stomach growth in the human fetal period: a post mortem study. *Int J Morphol.* 2012;30:461–6.
 135. Sase M, Asada H, Okuda M, Kato H. Fetal gastric size in normal and abnormal pregnancies. *Ultrasound Obstet Gynecol.* 2002;19:467–70.
 136. Hata T, Tanaka H, Noguchi J, Inubashiri E, Yanagihara T, Kondoh S. Three-dimensional sonographic volume measurement of the fetal stomach. *Ultrasound Med Biol.* 2010;36:1808–12.
 137. Ben-Haroush A, Yogev Y, Peled Y, Bar J, Hod M, Pardo J. Correlation between fetal gastric size and amniotic fluid volume. *J Clin Ultrasound.* 2005;33:119–22.
 138. Vierordt H. *Anatomische Physiologische Und Physikalische Daten Und Tabellen Zum Gebrauche Für Mediziner.* Jena: Verlag von Gustav Fischer; 1906.
 139. Touloukian RJ, Smith GJ. Normal intestinal length in preterm infants. *J Pediatr Surg.* 1983;18:720–3.
 140. Struijs MC, Diamond IR, de Silva N, Wales PW. Establishing norms for intestinal length in children. *J Pediatr Surg.* 2009;44:933–8.
 141. Shanklin DR, Cooke RJ. Effects of intrauterine growth on intestinal length in the human fetus. *Biol Neonate.* 1993;64:76–81.
 142. Marnerides A, Ghazi S, Sundberg A, Papadogiannakis N. Development of fetal intestinal length during 2nd-trimester in normal and pathologic pregnancies. *Pediatr Dev Pathol.* 2012;15:24–9.
 143. FitzSimmons J, Chinn A, Shepard TH. Normal length of the human fetal gastrointestinal tract. *Pediatr Pathol.* 1988;8:633–41.
 144. Desdicioglu K, Malas MA, Evcil EH. Development of the fetal duodenum: a postmortem study. *Fetal Diagn Ther.* 2009;26:16–23.
 145. Rao-Mohandas KG, Somayaji SN, Bairy KL, Nayak S, Vincent R. A study to evaluate the relationship between the age of the fetus and intestinal length. *Eur J Anat.* 2006;10:151–2.
 146. Weaver LT, Austin S, Cole TJ. Small intestinal length: a factor essential for gut adaptation. *Gut.* 1991;32:1321–3.
 147. Malas MA, Aslankoc R, Ungor B, Sulak O, Candir O. The development of jejunum and ileum during the fetal period. *Early Hum Dev.* 2003;74:109–24.
 148. Herlinger H. Anatomy of the small intestine. In: Herlinger H, Maglinte D, Birnbaum BAE, editors. *Clinical imaging of the small intestine.* 2nd ed. New York (NY): Springer-Verlag New York, Inc.; 1999. p. 3–12.
 149. Shah RS, Rajalakshmi R. Studies on human fetal tissues: I. Fetal weight and tissue weights in relation to gestational age, fetal size and maternal nutritional status. *Indian J Pediatr.* 1988;55:261–71.
 150. Ziliani M, Fernandez S. Correlation of ultrasonic images of fetal intestine with gestational age and fetal maturity. *Obstet Gynecol.* 1983;62:569–73.

151. Nyberg DA, Mack LA, Patten RM, Cyr DR. Fetal bowel: normal sonographic findings. *J Ultrasound Med.* 1987;6:3–6.
152. Malas MA, Aslankoc R, Ungor B, Sulak O, Candir O. The development of large intestine during the fetal period. *Early Hum Dev.* 2004;78:1–13.
153. Aoki S, Hata T, Senoh D, KM, Hata K, Takamiya O, et al. Ultrasonographic measurement of fetal colon. *Acta Neanatol Jpn.* 1989;25:559–62.
154. Goldstein I, Lockwood C, Hobbins JC. Ultrasound assessment of fetal intestinal development in the evaluation of gestational age. *Obstet Gynecol.* 1987;70:682–6.
155. Parulekar SG. Sonography of normal fetal bowel. *J Ultrasound Med.* 1991;10:211–20.
156. Malas MA, Gokcimen A, Sulak O. Growing of caecum and vermiform appendix during the fetal period. *Fetal Diagn Ther.* 2001;16:173–7.
157. Zalel Y, Perlitz Y, Gamzu R, Peleg D, Ben-Ami M. In-utero development of the fetal colon and rectum: sonographic evaluation. *Ultrasound Obstet Gynecol.* 2003;21:161–4.
158. Rubesova E, Vance CJ, Ringertz HG, Barth RA. Three-dimensional MRI volumetric measurements of the normal fetal colon. *AJR Am J Roentgenol.* 2009;192:761–5.
159. Clatworthy H Jr, Anderson RG. Development and growth of the human embryo and fetus: a graphic representation of some aspects. *Am J Dis Child.* 1944;67(3):167–75.
160. ICRP. Human alimentary tract model for radiological protection. *Ann ICRP.* 2006. <https://doi.org/10.1016/j.icrp.2006.03.001>.
161. Scammon RE. Some graphs and tables illustrating the growth of the human stomach. *Am J Dis Child.* 1919;17:395–422.
162. Hata K, Hata T, Kitao M. Ultrasonographic identification and measurement of the human fetal pancreas in utero. *Int J Gynaecol Obstet.* 1988;26:61–4.
163. Sampaio FJ. Analysis of kidney volume growth during the fetal period in humans. *Urol Res.* 1992;20:271–4.
164. Xu D, Chen M, Pan XL, Xia LP, Wang H. Dexamethasone induces fetal developmental toxicity through affecting the placental glucocorticoid barrier and depressing fetal adrenal function. *Environ Toxicol Pharmacol.* 2011;32:356–63.
165. Ping J, Wang JF, Liu L, Yan YE, Liu F, Lei YY, et al. Prenatal caffeine ingestion induces aberrant DNA methylation and histone acetylation of steroidogenic factor 1 and inhibits fetal adrenal steroidogenesis. *Toxicology.* 2014;321:53–61.
166. Sayed MM. Effect of prenatal exposure to nicotine/thiocyanate on the pituitary–adrenal axis of 1-month-old rat offspring. *Egypt J Histol.* 2016;39:307–16.
167. Viau M, Collin-Faure V, Richaud P, Ravanat JL, Candeias SM. Cadmium and T cell differentiation: limited impact in vivo but significant toxicity in fetal thymus organ culture. *Toxicol Appl Pharmacol.* 2007;223:257–66.
168. Holladay SD, Smith BJ. Fetal hematopoietic alterations after maternal exposure to benzo[a]pyrene: a cytometric evaluation. *J Toxicol Environ Health.* 1994;42:259–73.
169. Holladay SD, Luster MI. Alterations in fetal thymic and liver hematopoietic cells as indicators of exposure to developmental immunotoxicants. *Environ Health Perspect.* 1996;104(Suppl. 4):809–13.
170. Thayyil S, Cleary JO, Sebire NJ, Scott RJ, Chong K, Gunny R, et al. Post-mortem examination of human fetuses: a comparison of whole-body high-field MRI at 9.4 T with conventional MRI and invasive autopsy. *Lancet.* 2009;374:467–75.
171. Araujo Junior E, Nardoza LM, Rolo LC, Nowak PM, Filho JB, Moron AF. Reference range of embryo volume by 3-D sonography using the XI VOCAL method at 7 to 10 + 6 weeks of pregnancy. *Am J Perinatol.* 2010;27:501–5.
172. Kehl S, Kalk AL, Eckert S, Schaible T, Sutterlin M, Neff W, et al. Assessment of lung volume by 3-dimensional sonography and magnetic resonance imaging in fetuses with congenital diaphragmatic hernias. *J Ultrasound Med.* 2011;30:1539–45.
173. Strizek B, Cos Sanchez T, Khalife J, Jani J, Cannie M. Impact of operator experience on the variability of fetal lung volume estimation by 3D-ultrasound (VOCAL) and magnetic resonance imaging in fetuses with congenital diaphragmatic hernia. *J Matern Fetal Neonatal Med.* 2015;28(7):858–64.
174. Won HS, Lee SJ, Jun SM. Clinical application and usefulness of XI VOCAL in volume measurement [White paper]. Seoul: Medison Co, Ltd; 2006: 1–3.
175. Barreto EQ, Milani HJ, Haratz KK, Araujo Junior E, Nardoza LM, Moron AF. Reference intervals for fetal heart volume from 3-dimensional sonography using the extended imaging virtual organ computer-aided analysis method at gestational ages of 20 to 34 weeks. *J Ultrasound Med.* 2012;31:673–8.
176. Chang FM, Hsu KF, Ko HC, Yao BL, Chang CH, Yu CH, et al. Fetal heart volume assessment by three-dimensional ultrasound. *Ultrasound Obstet Gynecol.* 1997;9:42–8.
177. Cussen L, Scurry J, Mitropoulos G, McTigue C, Gross J. Mean organ weights of an Australian population of fetuses and infants. *J Paediatr Child Health.* 1990;26:101–3.
178. Gruenwald P, Hoang Ngoc M. Evaluation of body and organ weights in perinatal pathology. I. Normal standards derived from autopsies. *Am J Clin Pathol.* 1960;34:247–53.
179. Hansen K, Sung CJ, Huang C, Pinar H, Singer DB, Oyer CE. Reference values for second trimester fetal and neonatal organ weights and measurements. *Pediatr Dev Pathol.* 2003;6:160–7.
180. Marecki B. Changes in the weight of internal organs in the fetal ontogenesis. *Z Morphol Anthropol.* 1989;77:235–45.
181. Maroun LL, Graem N. Autopsy standards of body parameters and fresh organ weights in nonmacerated and macerated human fetuses. *Pediatr Dev Pathol.* 2005;8:204–17.
182. Mitropoulos G, Scurry J, Cussen L. Organ weight/bodyweight ratios: growth rates of fetal organs in the latter half of pregnancy with a simple method for calculating mean organ weights. *J Paediatr Child Health.* 1992;28:236–9.
183. Peralta CF, Cavoretto P, Csapo B, Falcon O, Nicolaides KH. Lung and heart volumes by three-dimensional ultrasound in normal fetuses at 12–32 weeks' gestation. *Ultrasound Obstet Gynecol.* 2006;27:128–33.
184. Phillips JB, Billson VR, Forbes AB. Autopsy standards for fetal lengths and organ weights of an Australian perinatal population. *Pathology.* 2009;41:515–26.
185. Schulz DM, Giordano DA, Schulz DH. Weights of organs of fetuses and infants. *Arch Pathol.* 1962;74:244–50.
186. Ozguner G, Sulak O, Koyuncu E. A morphometric study of suprarenal gland development in the fetal period. *Surg Radiol Anat.* 2012;34:581–7.
187. Singer DB, Sung CJ, Wigglesworth JS. Fetal growth and maturation: with standards for body and organ development. In: Wigglesworth JS, Singer DB, editors. *Textbook of fetal and perinatal pathology.* London: Blackwell Scientific Publications; 1991. p. 11–47.
188. Duncan KR, Issa B, Moore R, Baker PN, Johnson IR, Gowland PA. A comparison of fetal organ measurements by echo-planar magnetic resonance imaging and ultrasound. *BJOG.* 2005;112:43–9.
189. Gielecki J, Zurada A, Kozłowska H, Nowak D, Loukas M. Morphometric and volumetric analysis of the middle cerebral artery in human fetuses. *Acta Neurobiol Exp (Wars).* 2009;69:129–37.
190. Boito SM, Laudy JA, Struijk PC, Stijnen T, Wladimiroff JW. Three-dimensional US assessment of hepatic volume, head

- circumference, and abdominal circumference in healthy and growth-restricted fetuses. *Radiology*. 2002;223:661–5.
191. Casey ML, Carr BR. Growth of the kidney in the normal human fetus during early gestation. *Early Hum Dev*. 1982;6:11–4.
192. Jeanty P, Dramaix-Wilmet M, Elkhazen N, Hubinont C, van Regemorter N. Measurements of fetal kidney growth on ultrasound. *Radiology*. 1982;144:159–62.
193. Michielsen K, Meersschaert J, De Keyzer F, Cannie M, Deprest J, Claus F. MR volumetry of the normal fetal kidney: reference values. *Prenatal Diagn*. 2010;30:1044–8.
194. Tedesco GD, Bussamra LC, Araujo Junior E, Britto IS, Nardozza LM, Moron AF, et al. Reference range of fetal renal volume by three-dimensional ultrasonography using the VOCAL method. *Fetal Diagn Ther*. 2009;25:385–91.
195. van Vuuren SH, Damen-Elias HA, Stigter RH, van der Doef R, Goldschmeding R, de Jong TP, et al. Size and volume charts of fetal kidney, renal pelvis and adrenal gland. *Ultrasound Obstet Gynecol*. 2012;40:659–64.
196. Bahmaie A, Hughes SW, Clark T, Milner A, Saunders J, Tilling K, et al. Serial fetal lung volume measurement using three-dimensional ultrasound. *Ultrasound Obstet Gynecol*. 2000;16:154–8.
197. Gerards FA, Engels MA, Twisk JW, van Vugt JM. Normal fetal lung volume measured with three-dimensional ultrasound. *Ultrasound Obstet Gynecol*. 2006;27:134–44.
198. Moeglin D, Talmant C, Duyme M, Lopez AC. Fetal lung volumetry using two- and three-dimensional ultrasound. *Ultrasound Obstet Gynecol*. 2005;25:119–27.
199. Pohls UG, Rempfen A. Fetal lung volumetry by three-dimensional ultrasound. *Ultrasound Obstet Gynecol*. 1998;11:6–12.
200. Ruano R, Joubin L, Aubry MC, Thalabard JC, Dommergues M, Dumez Y, et al. A nomogram of fetal lung volumes estimated by 3-dimensional ultrasonography using the rotational technique (virtual organ computer-aided analysis). *J Ultrasound Med*. 2006;25:701–9.
201. Hata T, Kuno A, Dai SY, Inubashiri E, Hanaoka U, Kanenishi K, et al. Three-dimensional sonographic volume measurement of the fetal spleen. *J Obstet Gynaecol Res*. 2007;33:600–5.
202. Welcker H, Brandt A. Gewichtswerthe der Körper-organe bei dem Menschen und den Thieren: ein Beitrag zur vergleichenden Anatomie und Entwicklungsgeschichte. *Arch f Anthropol*. 1902;28:1–89.
203. Trotter M, Peterson RR. Weight of bone in the fetus: a preliminary report. *Growth*. 1968;32:83–90.
204. Ozguner G, Sulak O. Size and location of thyroid gland in the fetal period. *Surg Radiol Anat*. 2014;36(4):359–67.